Unbraced pallet rack design in accordance with European practice–Part 2: Essential verification checks

Claudio Bernuzzi [a,*], Armando Gobetti [b], Giammaria Gabbianelli [b], Marco Simoncelli [b]

[a] *Department of Architecture. Built Environment and Construction Engineering. Politecnico di Milano. Milano. Italy*
[b] *Department of Civil Engineering and Architecture. Università di Pavia. Pavia. Italy*

1. Introduction

This paper is the second part of a two-parts paper summarizing the preliminary outcomes of a study focused on the approaches currently adopted in Europe [1] to design steel storage pallet racks. In the first part [2] attention has been mainly focused on the selection of the method of analysis to evaluate internal forces and moments and few alternatives have been discussed. Several configurations of unbraced semi-continuous medium-rise racks, differing for the geometry, for the components and for the degree of stiffness of the joints (both beam-to-column and base-plate connections) were modeled. An open-source finite element (FE) analysis program [3,4] for academic use (Śiva) was used, to which Authors have implemented a refined beam formulation [5–7] able to capture adequately the response of mono-symmetric members commonly used in racks. In particular, the traditional FE beam formulation [8–10], typically characterized by 6 degrees of freedom (DOFs) per node, has been improved by adding the 7th DOF. i.e, the warping of the cross-section (θ), which is essential to model the eccentricity of the shear center with respect to the centroid (Fig. 1). To give a general overview of the cases frequently encountered in routine design, mono- and bi-symmetric cross-section uprights have been modeled, owing to the availability of both 6DOFs and 7DOFs FE beam formulations in Śiva. On the basis of overall elastic buckling analyses, it has been demonstrated that the alternatives offered to designers by European rack standard provisions, or not in contrast with them, could lead to critical load multipliers significantly different from each other, which influence directly the selection of the method of analysis. i.e, the choice between 1st or 2nd order elastic analysis.

In this second part of the paper, few design rules are discussed with reference to both serviceability and ultimate limit states [1,11]. Numerical applications are developed on the same set of racks already presented in the companion paper, to which reference can be made for all the input data related to the geometry of racks and components, as well as to the degree of flexural stiffness of both beam-to-column and base-plate joints, In Fig. 2, both the cross-aisle and the down-aisle views of the considered racks [2] are presented together with the three cross-sections of the uprights. Main results related to the elastic buckling analyses carried out by means of both 6DOFs and 7DOFs beam element formulations have been already discussed with reference to the selection of the method of analysis. Out-of-plumb was considered equal to 1/300 rad for both the down- and cross-aisle directions,

* Corresponding author.Tel.: +0223994246.
E-mail address: claudio.bernuzzi@polimi.it (C. Bernuzzi).

which has been simulated via additional horizontal forces. It is worth to mention that in routine design practice, out of plum imperfection is applied in each aisle as independent load case. It is authors' opinion that if the design is based on spatial rack models.

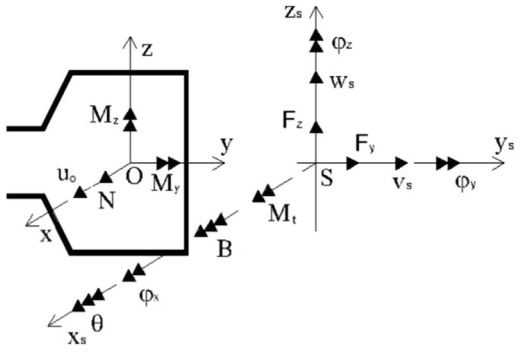

Fig. 1. The set of displacements and internal forces and moments for the finite element beam formulation with 7 DOFs per node.

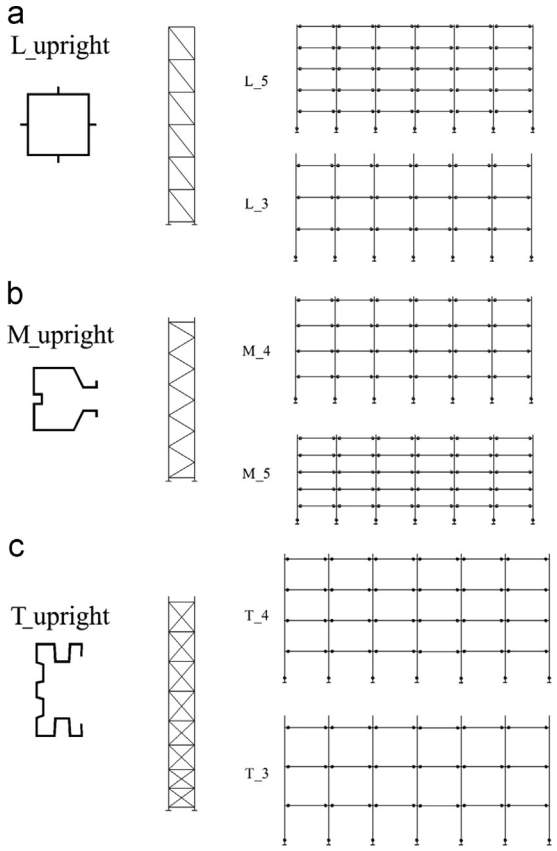

Fig. 2. Essential data of the L_, M_ and T_racks [2] considered in the numerical analysis.

imperfections have been considered in both the directions at the same time. Furthermore, it should be noted that the modest value of the considered out-of-plumb has a very negligible influence on the research outcomes. Procedures to evaluate the elastic critical load of isolated columns have been introduced and applied to adopt not only for the choice of the analysis method but also for the stability verification checks, as herein shown. The present paper deals with the safety of the different approaches, which can be adopted by rack designers, owing to the absence of a univocal procedure recommended by the European rack Code. For each rack, 2nd order elastic analysis have been carried out, differing for the values of the pallet load considered at the serviceability and at the ultimate limit states. In particular, the multiplier of the 6DOFs buckling analysis (α_{cr}^6) was used to define the serviceability load, assumed approximately equal to 0.4 times the value of pallet load activating the overall sway buckling of the rack ($\alpha_s = 0.4\alpha_{cr}^6$): it corresponds to a ratio between the critical load and the applied load in service equal to 2.5. Furthermore, considering the value of the amplifying load factor γ recommended by European Code for unit loads ($\gamma = 1.4$) in accordance with limit state design philosophy, the load condition at ultimate limit states was defined, which corresponds to 0.56 times ($\alpha_u = 0.56\alpha_{cr}^6$) the value of the elastic 6DOFs FE critical load multiplier (i.e. the ratio between the critical vertical load and the applied load on each rack is approximately 1.8 at the ultimate load condition). Other criteria should be adopted to define the service and ultimate load of the racks: furthermore, it should be noted that the research outcomes discussed in the following are independent on the applied load levels, being the scope of the paper a critical analysis associated with the results of the admitted design options.

Fig. 3 represents a summary of the verification checks herein considered, which regard to both the serviceability (overall deformability of the rack) and the ultimate limit states for uprights (resistance and stability).

2. Warping influence on the serviceability limit states

Attention has been at first focused on the warping effects of the lateral displacements, and hence only M_ and T_racks are considered, having the uprights with mono-symmetric cross-section. As to the serviceability load condition, reference is made to the 2nd order elastic displacement (δ) at the top of the rack in the down-aisle direction, which in the following is defined as δ^6 or δ^7 (the superscript indicates the number of DOFs adopted in the beam formulation). The influence of warping effects can be directly appraised via the ratio δ^7/δ^6, which is reported in Table 1. It can be noted that increasing the value of the beam-to-column joint stiffness, the 7DOFs displacement is greater than the corresponding 6DOFs one, up to 25% and 37% for M_4 and M_5 racks, respectively. In case of T_racks this influence is more limited, being not greater than 16%, but however not negligible. Furthermore, the influence of the base-plate connection stiffness is quite limited and generally the errors increase with the increase of $\rho_{j,base}$. It appears that the influence of the warping on the top lateral

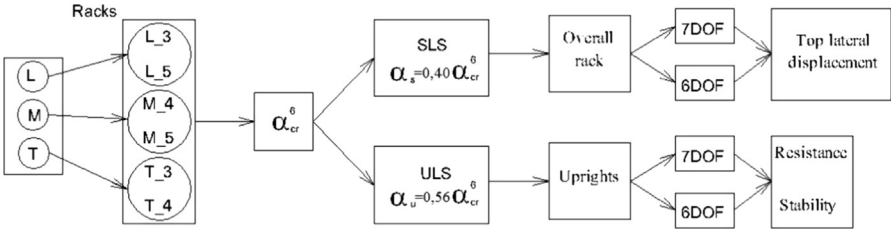

Fig. 3. Flow-charts of the upright verification checks in accordance with the considered design alternatives.

Table 1
Influence of the FE beam formulations on the top lateral displacements in the down-aisle direction.

δ^7/δ^6	$\rho_{j,btc}$	$\rho_{j,base}$			δ^7/δ^6	$\rho_{j,btc}$	$\rho_{j,base}$		
		0.15	0.30	0.45			0.15	0.30	0.45
Racks M_4	0.5	1.027	1.038	1.027	Racks T_3	0.5	1.050	1.050	1.054
	1.0	1.060	1.061	1.066		1.0	1.056	1.056	1.059
	1.5	1.085	1.090	1.089		1.5	1.062	1.062	1.065
	2.0	1.111	1.110	1.116		2.0	1.096	1.101	1.103
	3.5	1.152	1.160	1.167		3.5	1.113	1.119	1.122
	5.0	1.175	1.190	1.200		5.0	1.125	1.131	1.136
	7.0	1.196	1.217	1.229		7.0	1.137	1.144	1.149
	10.0	1.220	1.241	1.253		10.0	1.147	1.156	1.161
	mean	1.128	1.138	1.143		mean	1.098	1.102	1.106
Racks M_5	0.5	1.018	1.021	1.015	Racks T_4	0.5	1.039	1.044	1.045
	1.0	1.057	1.058	1.060		1.0	1.048	1.048	1.051
	1.5	1.090	1.095	1.097		1.5	1.053	1.056	1.058
	2.0	1.120	1.124	1.128		2.0	1.057	1.061	1.064
	3.5	1.184	1.199	1.205		3.5	1.072	1.079	1.082
	5.0	1.229	1.253	1.260		5.0	1.084	1.092	1.097
	7.0	1.267	1.300	1.313		7.0	1.094	1.105	1.110
	10.0	1.304	1.347	1.365		10.0	1.105	1.117	1.126
	mean	1.159	1.175	1.180		mean	1.069	1.075	1.079

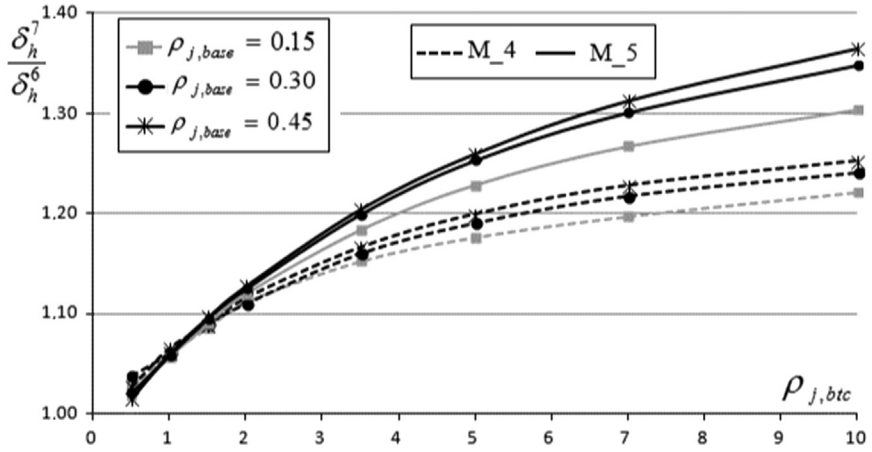

Fig. 4. $(\delta^7/\delta^6)-\rho_{j,btc}$ relationships for M_4 and M_5 racks.

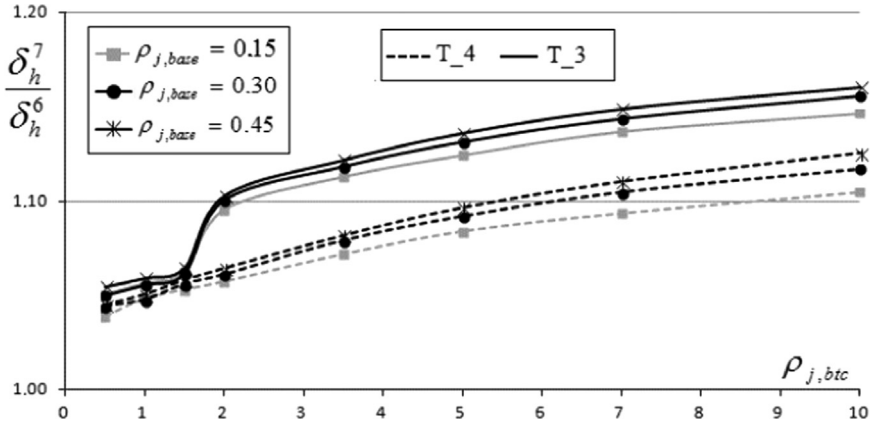

Fig. 5. $(\delta^7/\delta^6)-\rho_{j,btc}$ relationships for T_3 and T_4 racks.

displacements is non-negligible and the importance of suitable analysis tools is completely proved by Figs. 4 and 5 where the $\delta^7/\delta^6-\rho_{j,btc}$ relationships are presented for M_ and T_racks, respectively. Mean values of δ^7/δ^6 for each set of racks differing for the sole degree of beam-to-column joint stiffness range between 1.07 (T_3 with $\rho_{j,base}=0.15$) and 1.17 (M_5 with $\rho_{j,base}=0.45$). It should be noted that these remarks. proposed with reference to the maximum lateral displacement, are however totally proved, if the interstory drift associated to the different FE formulations is considered and compared.

It is worth to mention that the influence of warping is expected to be very relevant also for pallet beams. In several cases, lipped

channels are used, which are interested in torsional deformations as well as in a severe state of stresses due to the warping torsion [12–13]. European rack provisions limit the maximum vertical deflection of the pallet beams but recommend also a value of 6 degrees as the maximum twist admitted for the pallet beams. As a consequence when lipped channels are used, the pallets are supported by the upper cross-section flange and a remarkable influence on the vertical displacement is expected, due to the eccentricity of the load application point with respect to the shear center. Serviceability limit states for pallet beams are not herein considered, but authors are working on this topic investigating the response of mono- and non-symmetric cross section beams with reference to the vertical displacement as well as to the twisting rotation [14].

3. Warping influence on the structural analysis results

As discussed in the previous ssection, the influence of warping effects on the results of the structural analysis can be herein appraised with reference to M_ and T_racks, being these ones realized with mono-symmetric upright cross-sections. Warping effects influence remarkably all the output parameters and in particular, the complete set of internal forces and moments on each member of the racks. As to axial load (N), no significant differences between 6DOFs and 7DOFs results have been observed, which have been instead noted for the shear forces (F_y and F_z), despite the fact that generally they do not govern rack design. As to bending moments M_y and M_z, in the down- and cross-aisle directions, respectively, a summary of the differences between 6DOFs (apex 6) and 7DOFs (apex 7) FE results related to the more stressed internal (C.U.) and external (E.U.) uprights can be directly appraised via Table 2 (M_y^7/M_y^6). and Table 3 (M_z^7/M_z^6).

If the down-aisle moments are considered, ratio M_y^7/M_y^6 of the internal uprights is slightly greater than the one associated with the E.U. and it results in value always greater than unity except in case of M_5 racks with $\rho_{j.btc}=0.5$. In particular, if M_5 and T_racks are considered, the maximum differences between M_y^7 and M_y^6 are limited to 25% for the internal and 9% for the external uprights. Otherwise, in case of M_4 racks, these differences are very important, ranging from 2.5 to 3.6 and from 1.9 to 2.5 for C.U and E.U., respectively. Furthermore. Figs. 6 and 7 present the $M_y^7/M_y^6-\rho_{j,btc}$ relationships for the more stressed uprights of M_4 and T_3 racks. Ratio M_y^7/M_y^6 increases always with the increase of $\rho_{j,btc}$ for both C.U. and E.U., except for the E.U. of the M_4 racks. With reference to the cross-aisle moments, the influence of warping effects appears always significantly greater than the one for the down-aisle moments, with the exception of M_ 4 racks, where M_z^7/M_z^6 is in general slightly lower than unity for C.U. and for the E.U. slightly greater than unity. In case of M_5 racks, the ratio M_z^7/M_z^6 ranges approximately for C.U. between 4.5 and 5.2 and for E.U. between 4.4 and 4.7. Otherwise, for T_3 and T_5 racks M_z^7/M_z^6 is approximately constant and equal to 1.3.

As a general conclusion the great dispersion of these ratios should be noted. If reference is made to the bending moments in the down-aisle direction (M_y). Fig. 8 presents the frequency and cumulated relative frequency of ratio M_y^7/M_y^6 for the more stressed C.U. of each rack with mono-symmetric uprights: the 95% fractile value is approximately equal to 3.3. Mean value of M_y^7/M_y^6 for each set of similar racks (i.e, racks differing only for the sole value of the beam-to-column joint stiffness) is generally lower than 1.1, except for M_4 racks, ranging between 2.1 and 3.3. Similarly, no general rules can be deduced about the warping influence on the moments in the cross-aisle direction: mean value of M_z^7/M_z^6 ranges between 0.93 and 1.32 except for M_5 racks, ranging between 4.6 and 4.9. Fig. 9 presents the frequency and the cumulated relative frequency of M_z^7/M_z^6: the peak of distribution in correspondence of the value of approximately 1.3 is due to T_racks. Furthermore, a relevant number of cases with errors greater than 4.0 (M_5 racks) can be noted and this leads to a very high value of the 95% fractile value (approximately equal to 4.9).

Table 2
Influence of the warping effects on the bending moments in the down-aisle direction (M_y) for the more stresses internal (C.U.) and external (E.U.) upright.

M_y^7/M_y^6	$\rho_{j,btc}$	C.U.: $\rho_{j,base}$			E.U.: $\rho_{j,base}$		
		0.15	0.30	0.45	0.15	0.30	0.45
Racks M_4	0.5	2.740	2.588	2.534	2.517	2.390	2.347
	1.0	2.964	2.762	2.709	2.487	2.287	2.243
	1.5	3.150	2.906	2.836	2.452	2.251	2.153
	2.0	3.263	3.041	2.926	2.385	2.205	2.107
	3.5	3.525	3.271	3.149	2.294	2.102	2.031
	5.0	3.614	3.404	3.275	2.232	2.066	1.978
	7.0	3.619	3.441	3.322	2.149	2.011	1.938
	10.0	3.621	3.440	3.364	2.087	1.965	1.910
	mean	3.312	3.107	3.015	2.325	2.160	2.088
Racks M_5	0.5	0.989	0.984	0.980	0.991	0.992	0.992
	1.0	1.017	1.012	1.012	1.013	1.009	1.011
	1.5	1.053	1.049	1.045	1.036	1.034	1.030
	2.0	1.080	1.072	1.071	1.051	1.048	1.045
	3.5	1.135	1.143	1.142	1.070	1.071	1.065
	5.0	1.168	1.183	1.183	1.075	1.078	1.078
	7.0	1.190	1.210	1.216	1.075	1.080	1.082
	10.0	1.208	1.236	1.244	1.070	1.081	1.088
	mean	1.105	1.111	1.112	1.048	1.049	1.049
Racks T_3	0.5	1.051	1.050	1.055	1.046	1.047	1.040
	1.0	1.061	1.068	1.062	1.056	1.051	1.051
	1.5	1.078	1.078	1.077	1.061	1.053	1.051
	2.0	1.088	1.091	1.085	1.064	1.056	1.056
	3.5	1.113	1.114	1.111	1.074	1.064	1.060
	5.0	1.130	1.129	1.130	1.078	1.068	1.066
	7.0	1.144	1.144	1.148	1.081	1.069	1.067
	10.0	1.158	1.158	1.157	1.081	1.071	1.069
	mean	1.103	1.104	1.103	1.068	1.060	1.058
Racks T_4	0.5	1.031	1.035	1.035	1.023	1.026	1.025
	1.0	1.040	1.041	1.042	1.030	1.029	1.032
	1.5	1.051	1.050	1.049	1.039	1.033	1.032
	2.0	1.064	1.060	1.058	1.045	1.039	1.034
	3.5	1.085	1.079	1.080	1.052	1.041	1.041
	5.0	1.097	1.096	1.091	1.055	1.046	1.043
	7.0	1.111	1.108	1.107	1.055	1.048	1.043
	10.0	1.121	1.120	1.117	1.058	1.049	1.044
	mean	1.075	1.074	1.072	1.045	1.039	1.037

No prediction of warping effects via simplified techniques appears possible: in several cases, differences between M^7/M^6 are very big and, as a consequence, a non-negligible influence of warping is expected on the values of the safety index: the only way to obtain correct input design values for the verification checks is inevitably to use suitable 7DOFs beam element formulations.

4. Warping influence on the upright resistance

Modern design codes are based on main verification checks on the evaluation of a safety index (SI), which are fulfilled if $SI \leq 1$, and for routine rack design SI is always associated with the use of 6DOFs beam formulations. Owing to the fact that all the upright cross-sections herein considered belong to class 3 in accordance with the European classification criteria [15], the corresponding resistance safety index (SI_G^6) is referred to the global properties of the cross-section in terms of axial (N_{Rd}) and bending resistance ($M_{y,Rd}$ and $M_{z,Rd}$) and it is defined as:

$$SI_G^6 = \frac{N_{Ed}}{N_{Rd}} + \frac{M_{y,Ed}}{M_{y,Rd}} + \frac{M_{z,Ed}}{M_{z,Rd}} = \frac{N_{Ed}}{f_y A} + \frac{M_{y,Ed}}{f_y I_y} z_{\max} + \frac{M_{z,Ed}}{f_y I_z} y_{\max} \quad (1)$$

where f_y is the material yielding strength, A and I are the area and the second moment of area of the cross-section, respectively, and subscripts y and z are referred to the principal axes of the cross-section.

It should be noted that the bending resistance ($M_{y,Rd}$ and $M_{z,Rd}$) has been evaluated with reference to the elastic cross-section moduli $I_y/z_{max}$and I_z/y_{max}.

In case of beam formulations including warping effects, the global resistance safety index (SI_G^7) has necessarily to be taken into account for the bi-moment contribution, also as recommended by the very recently updated Australian standards [16] as well. In accordance with the criteria associated with Eq. (1), an appropriate safety index for the resistance verification of mono-symmetric cross-section members (SI_G^7) should be necessarily defined as

$$SI_G^7 = SI_G^{6(7)} + SI_G^{BM(7)} = SI_G^{6(7)} + \frac{B_{Ed}}{B_{Rd}} \tag{2}$$

where $SI_G^{6(7)}$ is the safety index evaluated on the basis of Eq. (1)) but using the values of internal forces and bending moments arising from a 7DOFs FE analysis generally greater than the one associated with 6DOFs. $SI_G^{BM(7)}$ is the SI contribution due to the presence of the design bi-moment and B_{Rd}bi-moment cross-section resistance, defined as

$$B_{Rd} = \frac{I_w}{\omega_{max}} f_y \tag{3}$$

where I_w is the warping constant and ω_{max} is the maximum value of the static moment of the sectorial area, in accordance with the well-established theory [12,13] or with simplified procedure proposed in Appendix A of the present paper.

Table 3
Influence of the warping effects on the bending moments in the down-aisle direction (M_z) for the more stresses internal (C.U.) and external (E.U.) upright.

M_z^7/M_z^6	$\rho_{j,btc}$	C.U.: $\rho_{j,base}$			E.U.: $\rho_{j,base}$		
		0.15	0.30	0.45	0.15	0.30	0.45
Racks M_4	0.5	0.962	0.913	1.010	0.946	0.899	1.104
	1.0	0.976	0.923	0.980	0.960	1.061	1.039
	1.5	0.925	0.931	0.973	1.043	0.979	0.960
	2.0	0.929	0.971	0.951	1.033	1.067	1.046
	3.5	0.940	0.946	0.960	1.033	1.031	1.001
	5.0	0.937	0.921	0.928	1.030	1.005	1.047
	7.0	0.954	0.919	0.918	1.052	1.007	1.039
	10.0	0.938	0.927	0.918	1.005	1.023	1.044
	mean	0.945	0.931	0.955	1.013	1.009	1.035
Racks M_5	0.5	4.710	4.545	4.483	4.698	4.545	4.487
	1.0	4.680	4.739	4.684	4.525	4.348	4.721
	1.5	4.810	4.798	4.726	4.745	4.530	4.452
	2.0	4.729	4.858	4.785	4.747	4.518	4.451
	3.5	4.802	4.947	4.856	4.738	4.695	4.608
	5.0	4.974	5.018	4.924	4.656	4.742	4.637
	7.0	4.976	5.072	5.065	4.665	4.673	4.736
	10.0	5.045	5.181	5.152	4.717	4.647	4.682
	mean	4.841	4.895	4.834	4.686	4.587	4.597
Racks T_3	0.5	1.297	1.355	1.331	1.277	1.335	1.312
	1.0	1.345	1.302	1.318	1.374	1.284	1.345
	1.5	1.313	1.331	1.335	1.297	1.352	1.320
	2.0	1.309	1.336	1.330	1.295	1.323	1.350
	3.5	1.319	1.325	1.333	1.315	1.295	1.304
	5.0	1.314	1.320	1.315	1.319	1.325	1.321
	7.0	1.335	1.316	1.325	1.297	1.330	1.318
	10.0	1.321	1.328	1.329	1.295	1.310	1.334
	mean	1.319	1.327	1.327	1.309	1.319	1.325
Racks T_4	0.5	1.328	1.325	1.303	1.364	1.304	1.283
	1.0	1.319	1.328	1.308	1.299	1.309	1.288
	1.5	1.314	1.333	1.307	1.295	1.345	1.320
	2.0	1.332	1.330	1.328	1.343	1.315	1.338
	3.5	1.308	1.313	1.321	1.322	1.307	1.316
	5.0	1.314	1.312	1.310	1.334	1.331	1.329
	7.0	1.310	1.314	1.320	1.301	1.308	1.300
	10.0	1.319	1.315	1.311	1.321	1.306	1.317
	mean	1.318	1.321	1.314	1.322	1.316	1.311

4.1. Numerical applications

Table 4 represents the values of the ratios SI_G^7/SI_G^6 for the more stressed internal (C.U.) and external (E.U.) uprights together with the associated standard deviation and the maximum value of this ratio. No big difference can be observed between the C.U. and E.U. values, except than for M_4 racks where the warping effects are slightly greater in E.U., with SI_G^7/SI_G^6 up to 1.45. than in C.U., with SI_G^7/SI_G^6 up to 1.27. Otherwise. if reference is made to M_5 racks. the values of the ratio SI_G^7/SI_G^6 are slightly greater than unity (up to 1.1) despite the great differences previously observed in the ratio M_z^7/M_z^6, owing to the limited influence on resistance checks of the bending moment M_z acting in the cross-aisle direction. Similar values observed for M_4 racks can be also noted also in both T_3 and T_5 racks. As an example, Fig. 10 can be considered, where the ratio SI_G^7/SI_G^6 is plotted versus $\rho_{j,btc}$ for M_4 racks. It can be noted that the influence of warping effects is more relevant for the more stressed external uprights, which decreases with the increase of stiffness joints; otherwise, this ratio for C.U. is quite constant (approximately equal to 1.25) and it appears to be practically independent from the joint stiffness. A statistical evaluation SI_G^7/SI_G^6 can be appraised via Fig. 11, where the frequency and cumulated relative frequency are reported: a great concentration of the data is in the range 1.05–1.26 and the 95% fractile value is approximately equal to 1.4.

It should be noted that the differences from unity of the ratio $SI_G^7/SI_G^6$are mainly due to 1) the different values of the bending

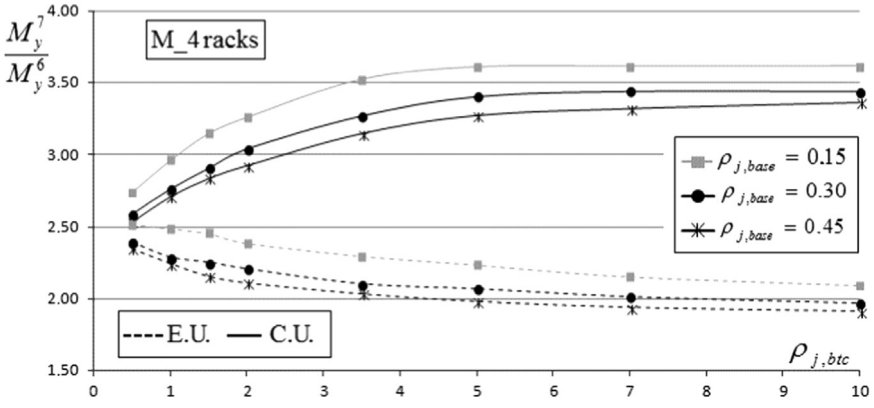

Fig. 6. $M_y^7/M_y^6 - \rho_{j,btc}$ relationships for the more stressed internal (C.U.) and external (E.U.) uprights of M_4 racks.

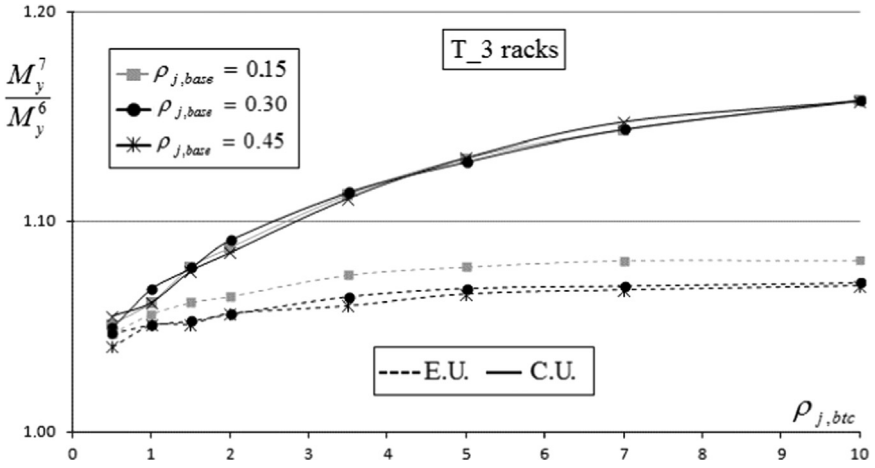

Fig. 7. : $M_y^7/M_y^6 - \rho_{j,btc}$ relationships for the more stressed internal (C.U.) and external (E.U.) uprights of T_3 racks.

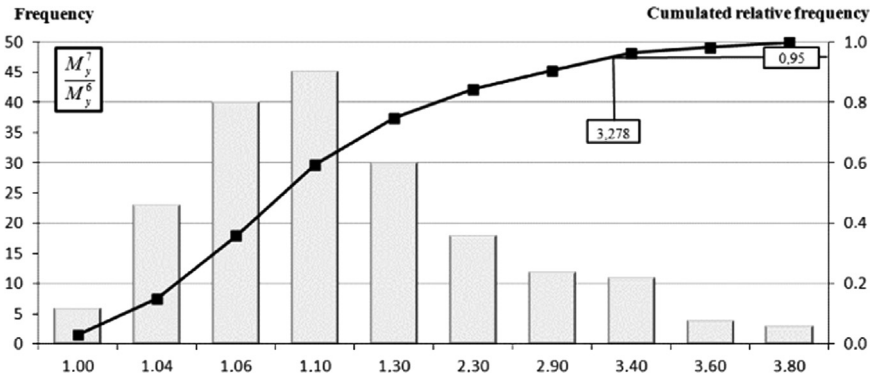

Fig. 8. Frequency and cumulated relative frequency of ratio M_y^7/M_y^6 for M_ and _T racks. for the more stressed central upright.

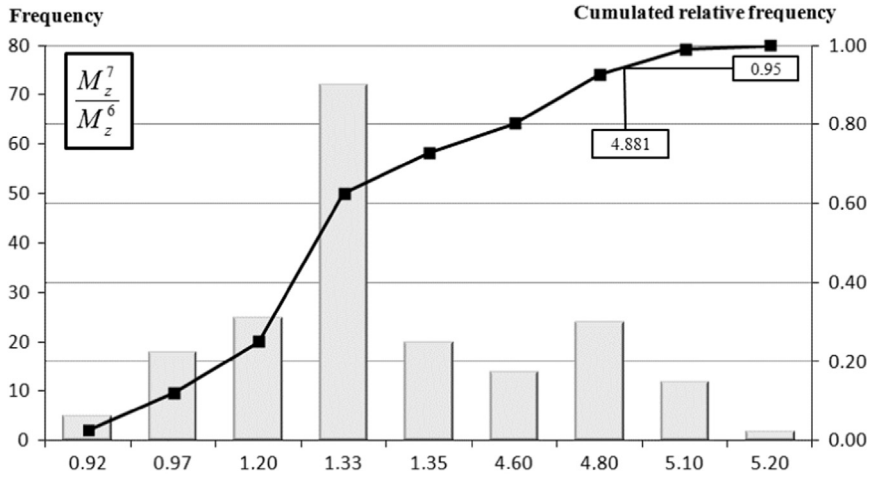

Fig. 9. Frequency and cumulated relative frequency of ratio M_z^7/M_z^6 for M_ and _T racks. for the more stressed central upright.

moments M_y and M_z associated with a 6DOFs and a 7DOFs structural analysis and 2) the presence of the bi-moment in the verification check proposed by Eq. (2) The first contribution is a direct consequence of the 2nd order elastic analysis required to account for the lateral rack deformability. The geometric stiffness matrix, as reported in Appendix A of the companion paper [2], includes terms directly associated with bending and torsional moments. As a consequence, neglecting the warping, as well limited differences in the safety index, is expected, depending on the type of the beam formulation adopted. To this purpose, reference can be made to Table 5, which presents the ratio $SI_G^{6(7)}/SI_G^6$, i.e, the ratio between the safety index in Eq. (1) evaluated by considering the bending moments arising from a 7DOFs FE analysis ($SI_G^{6(7)}$) and the one obtained via a moment distribution based on a 6DOFs analysis (SI_G^6). It can be noted that $SI_G^{6(7)}/SI_G^6$ is generally quite constant or moderately decreasing with the increase of $\rho_{j,btc}$. For M_4 racks $SI_G^{6(7)}$ is significantly greater than SI_G^6, up to 25% and 41% for C.U. and E.U., respectively. Otherwise, this ratio is slightly greater than unity except for M_5 racks, where, especially for E.U, the safety index obtained via a 7DOFs analysis is lower than the one associated with the 6DOFs one. It should be noted that only for these cases, a traditional

analysis software is from the safe side. In Figs. 12 and 13 both the $SI_G^7/SI_G^6-\rho_{j,btc}$ and $SI_G^{6(7)}/SI_G^6-\rho_{j,btc}$ relationships are directly compared for the central uprights of M_4 and M_5 racks. respectively. to allow better appraisal of the importance of the FE element beam formulations. Furthermore. in order to single out the influence of the bi-moment on the safety index. Table 6 presents the contribution due to the bi-moment in terms of safety index ratio $SI_G^{BM(7)}$ over SI_G^7. For the M_4 racks the values of the ratio $SI_G^{BM(7)}/SI_G^7$ are quite limited. up to 0.09 for C.U. and 0.10 for E.U.; on the other hand. if reference is made to M_5 racks. $SI_G^{BM(7)}$ contributes significantly to the global value of SI_G^7: up to 16% and 29% for C.U. and E.U., respectively. In case of T_racks bi-moment influence is very limited and its contribution to the resistance safety index is never greater than 3%. Owing to the importance of the bi-moment contribution on the resistance cross-section safety index, the ratio $SI_G^{BM(7)}/SI_G^7$ has been plotted versus $\rho_{j,btc}$ in Fig. 14 (M_4 racks) and Fig. 15 (M_5 racks). The trends are qualitatively similar for both racks: increasing the joint stiffness the slope of the curves decreases, more rapidly for C.U. than for E.U.; the greatest differences can be observed in M_5 racks. In Fig. 16 the frequency and cumulated relative frequency of ratio $SI_G^{BM(7)}/SI_G^7$ are plotted for all the more stressed internal uprights for each of the M_ and T_racks: a very relevant concentration of data can be noted up to 0.10 but the fractile value of the ratio is however very high, approximately 0.23.

Table 4
Influence of the warping effects on the safety index associated with the cross-section resistance for the more stresses internal (C.U.) and external (E.U.) upright.

SI_G^7/SI_G^6	$\rho_{j,btc}$	C.U.: $\rho_{j,base}$			E.U.: $\rho_{j,base}$		
		0.15	0.30	0.45	0.15	0.30	0.45
Racks M_4	0.5	1.268	1.253	1.256	1.446	1.431	1.440
	1.0	1.256	1.240	1.242	1.420	1.401	1.398
	1.5	1.253	1.240	1.240	1.418	1.391	1.373
	2.0	1.252	1.247	1.238	1.403	1.391	1.372
	3.5	1.261	1.254	1.249	1.393	1.375	1.365
	5.0	1.261	1.260	1.254	1.384	1.373	1.361
	7.0	1.259	1.260	1.256	1.369	1.364	1.355
	10.0	1.256	1.260	1.260	1.353	1.356	1.353
	mean	1.258	1.252	1.249	1.398	1.385	1.377
	max	1.268	1.260	1.260	1.446	1.431	1.440
Racks M_5	0.5	1.050	1.046	1.044	1.038	1.036	1.035
	1.0	1.060	1.059	1.059	1.047	1.043	1.048
	1.5	1.071	1.070	1.068	1.060	1.056	1.053
	2.0	1.076	1.076	1.075	1.065	1.061	1.059
	3.5	1.089	1.093	1.091	1.072	1.072	1.068
	5.0	1.099	1.102	1.100	1.072	1.074	1.073
	7.0	1.103	1.108	1.109	1.071	1.073	1.075
	10.0	1.108	1.115	1.116	1.068	1.073	1.077
	mean	1.082	1.084	1.083	1.062	1.061	1.061
	max	1.108	1.115	1.116	1.072	1.074	1.077
Racks T_3	0.5	1.052	1.059	1.057	1.048	1.054	1.049
	1.0	1.061	1.057	1.057	1.062	1.051	1.057
	1.5	1.061	1.063	1.063	1.056	1.058	1.055
	2.0	1.062	1.067	1.065	1.057	1.057	1.060
	3.5	1.069	1.071	1.071	1.064	1.058	1.057
	5.0	1.072	1.073	1.073	1.066	1.062	1.061
	7.0	1.077	1.075	1.078	1.065	1.063	1.062
	10.0	1.078	1.080	1.080	1.065	1.062	1.064
	mean	1.066	1.068	1.068	1.060	1.058	1.058
	max	1.078	1.080	1.080	1.066	1.063	1.064
Racks T_4	0.5	1.050	1.051	1.048	1.047	1.042	1.039
	1.0	1.052	1.054	1.051	1.044	1.044	1.044
	1.5	1.054	1.057	1.053	1.047	1.050	1.047
	2.0	1.060	1.059	1.058	1.055	1.050	1.050
	3.5	1.061	1.060	1.062	1.055	1.049	1.050
	5.0	1.064	1.063	1.062	1.057	1.054	1.052
	7.0	1.065	1.066	1.066	1.053	1.052	1.049
	10.0	1.068	1.068	1.067	1.056	1.051	1.051
	mean	1.059	1.060	1.058	1.052	1.049	1.048
	max	1.068	1.068	1.067	1.057	1.054	1.052

It should be noted that the verification checks carried out via Eq. (2) should result slightly conservative. As already observed by Bernuzzi et al. [17], in case of bi-symmetric cross-section. Eq. (1) is related to the evaluation of the maximum normal stress in the cross-section. Otherwise, if warping contribution (bi-moment) is included in the evaluation of the safety index, the point where the stress due to bi-moment (σ_w) is maximum does not coincide with the point where the stresses due to axial force (σ_N), and bending moments (σ_{My} and σ_{Mz}) cumulate each other unfavorably. As an example, Figs. 17 and 18 can be considered, related to the M_ and T_ cross-sections, respectively, where, for the key points of the cross-section defining its perimeter, the dimensionless values of the normal stresses associated with bending moments $\sigma_y(y,z)/\sigma_{y,\max}$ and $\sigma_z(y,z)/\sigma_{z,\max}$ and bi-moment $\sigma_\omega(y,z)/\sigma_{\omega,\max}$ are presented. The former two ratios can be easily obtained via the de Saint Venant theory, while the term $\sigma_\omega(y,z)$, with which steel designers are less familiar, can be accessed via the expression:

$$\sigma_\omega(y,z)=\frac{B}{I_W}\omega(y,z) \tag{4}$$

where ω (y,z) is the sectorial area.

Distribution of ω (y,z). in accordance with the approach proposed in Appendix A, and hence of the normal warping stresses $\sigma_\omega(y,z)$, is reported in Figs. 17 and 18 for the considered mono-symmetric cross-sections. It can be noted that the points where the warping stresses are maximum/minimum are in correspondence of points B (and B′) and A (and A′), for M_ and T_racks, respectively. Otherwise, the sum of the sole stress due to axial load and bending moments is maximum in correspondence of point F′ (M_upright) or G′ (T_upright), confirming the potential overestimation of the maximum stress via Eq. (2).

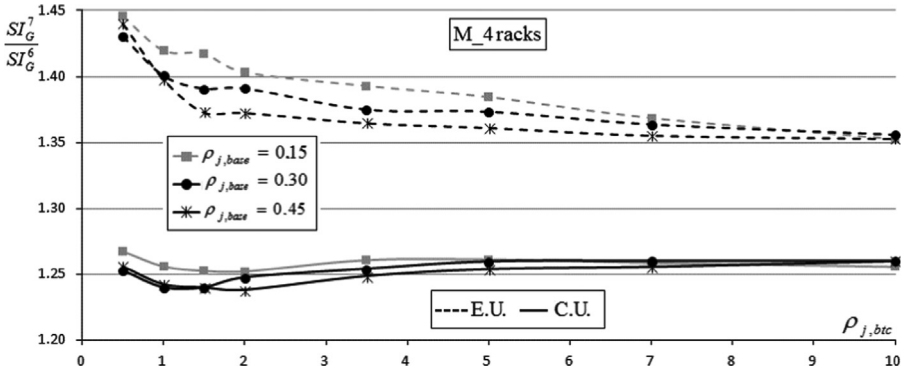

Fig. 10. $SI_G^7/SI_G^7-\rho_{j,btc}$ relationships for the more stressed internal (C.U.) and external (E.U.) uprights in M_4 racks.

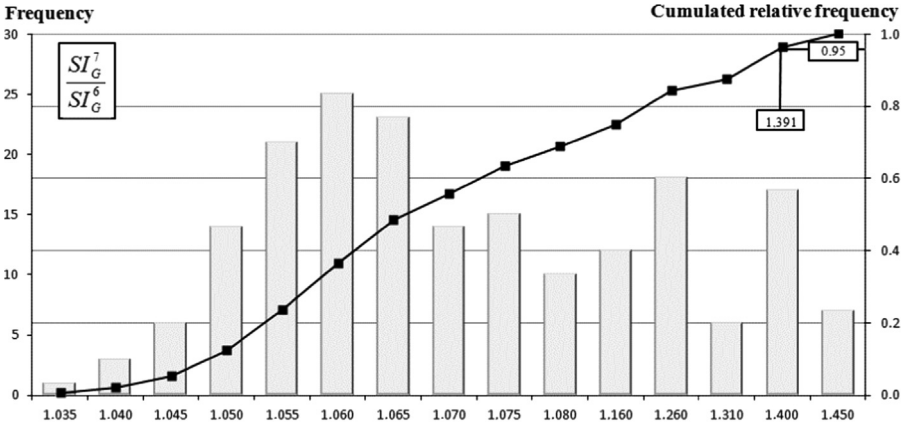

Fig. 11. Frequency and cumulated relative frequency of ratio SI_G^7/SI_G^7 for M and T racks, for the more stressed central upright.

Table 5
Influence of the FE beam formulation on the resistance verification checks via Eq. (1). i.e, by considering only the axial force and bending moments and neglecting the bi-moment contribution.

$SI_G^{6(7)}/SI_G^6$	$\rho_{j,btc}$	C.U.: $\rho_{j,base}$			E.U.: $\rho_{j,base}$		
		0.15	0.30	0.45	0.15	0.30	0.45
Racks M_4	0.5	1.248	1.216	1.220	1.414	1.401	1.411
	1.0	1.202	1.189	1.181	1.353	1.340	1.339
	1.5	1.194	1.168	1.158	1.327	1.310	1.279
	2.0	1.193	1.166	1.150	1.309	1.293	1.264
	3.5	1.197	1.160	1.143	1.279	1.254	1.239
	5.0	1.196	1.162	1.141	1.258	1.237	1.223
	7.0	1.198	1.159	1.141	1.240	1.221	1.213
	10.0	1.198	1.159	1.142	1.221	1.213	1.205
	mean	1.204	1.172	1.161	1.300	1.283	1.272
	max	1.248	1.216	1.220	1.414	1.401	1.411
Racks M_5	0.5	1.006	1.004	1.002	0.972	0.957	0.958
	1.0	0.998	0.992	0.993	0.920	0.911	0.919
	1.5	0.995	0.991	0.984	0.899	0.888	0.889
	2.0	0.993	0.981	0.981	0.877	0.871	0.866
	3.5	0.988	0.973	0.966	0.834	0.827	0.826
	5.0	0.989	0.968	0.959	0.810	0.802	0.801
	7.0	0.988	0.961	0.947	0.791	0.784	0.782
	10.0	0.991	0.956	0.939	0.774	0.763	0.763
	mean	0.994	0.978	0.971	0.860	0.850	0.850
	max	1.006	1.004	1.002	0.972	0.957	0.958
Racks T_3	0.5	1.052	1.041	1.040	1.048	1.054	1.049
	1.0	1.048	1.045	1.045	1.062	1.051	1.057
	1.5	1.050	1.043	1.044	1.040	1.043	1.040
	2.0	1.052	1.049	1.047	1.043	1.044	1.047
	3.5	1.053	1.048	1.042	1.052	1.037	1.037
	5.0	1.057	1.046	1.047	1.055	1.043	1.043
	7.0	1.063	1.050	1.047	1.054	1.046	1.045
	10.0	1.064	1.056	1.051	1.055	1.046	1.041
	mean	1.055	1.047	1.046	1.051	1.045	1.045
	max	1.064	1.056	1.051	1.062	1.054	1.057
Racks T_4	0.5	1.035	1.037	1.034	1.047	1.042	1.039
	1.0	1.042	1.034	1.031	1.028	1.029	1.029
	1.5	1.037	1.040	1.029	1.034	1.038	1.035
	2.0	1.044	1.037	1.037	1.043	1.028	1.028
	3.5	1.042	1.037	1.033	1.036	1.032	1.025
	5.0	1.041	1.038	1.032	1.040	1.031	1.030
	7.0	1.045	1.038	1.035	1.038	1.031	1.023
	10.0	1.049	1.038	1.034	1.042	1.026	1.027
	mean	1.042	1.037	1.033	1.038	1.032	1.029
	max	1.049	1.040	1.037	1.047	1.042	1.039

5. Upright stability checks

As to the stability checks in accordance with the European design approach, reference can be at first made to members subjected to the sole design axial force N_{Ed}. The following condition has to be fulfilled:

$$\frac{N_{Ed}}{\chi_{\min} A_{eff} f_y/(\gamma_M)} \leq 1 \tag{5}$$

where A_{eff} is the effective area, f_y is the yielding strength, χ_{min} is the design reduction resistance factor and γ_M is the material safety factor.

Reduction factor χ_{min} is the smallest between the reduction factors associated with distortional (χ_{db}), flexural (χ_y and χ_z) and flexural–torsional (χ_{FT}) or torsional (χ_T) buckling modes (if cross-section has one axis of symmetry, χ_{FT} has to be considered, otherwise when there are two axes of symmetry, χ_T has to be used).

It is worth to mention that all the cross-sections herein considered are in class 3 [15], i.e. the effective properties are coincident with the gross ones (A_{eff}=A) and as a consequence the distortional buckling is never critical. Reduction factor χ is defined as:

$$\chi = \frac{1}{\{0.5\,[1+0.34(\bar{\lambda}-0.2)+\bar{\lambda}^2]\}+\sqrt{\{0.5\,[1+0.34(\bar{\lambda}-0.2)+\bar{\lambda}^2]\}^2-\bar{\lambda}^2}} \leq 1 \tag{6}$$

Relative slenderness $\bar{\lambda}$ depends strictly on the elastic critical load for the appropriate buckling mode (N_{cr}), being defined as:

$$\bar{\lambda} = \sqrt{\frac{A f_y}{N_{cr}}} \tag{7}$$

The case of pure axial load is extremely rare in rack design practice and it is generally associated with the verification of lacings, With reference to the uprights, in addition to the contribution due to axial load, it is of fundamental importance to take into account also the presence of bending moments along the principal axes of the cross-section, which, as previously discussed, are significantly influenced by the deformability of the rack to lateral loads and by the FE formulation adopted for structural analysis. Uprights are generally beam–column members subjected to axial load N_{Ed} and to bending moments along the principal cross-section axes, $M_{y,Ed}$ and $M_{z,Ed,}$ where pedix y identifies the major axis (in these cases the symmetry axis). Owing to the use of open cross-sections, uprights are usually interested by lateral torsional buckling and, with reference to stability checks, the

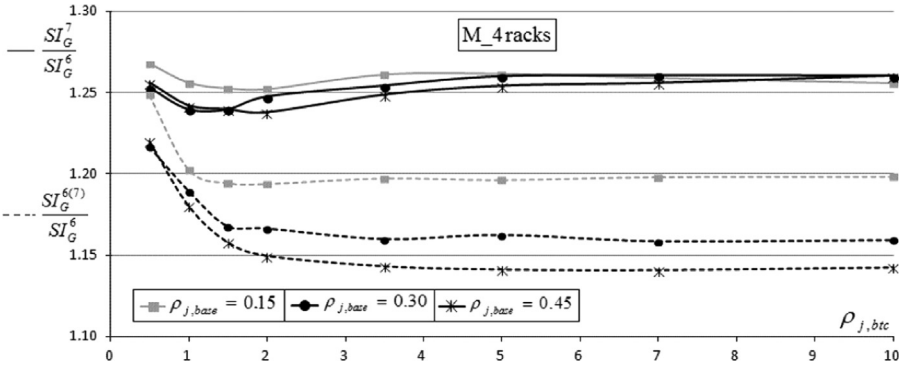

Fig. 12. $SI_G^7/SI_G^7-\rho_{j,btc}$ *and* $SI_G^{6(7)}/SI_G^7-\rho_{j,btc}$ relationships for M_4 racks.

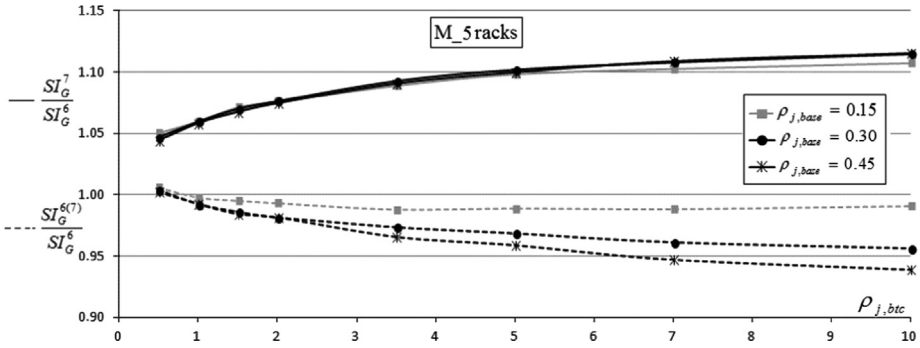

Fig. 13. $SI_G^7/SI_G^7-\rho_{j,btc}$ *and* $SI_G^{6(7)}/SI_G^7-\rho_{j,btc}$ relationships for M_5 racks.

following condition has to be fulfilled:

$$\left(\frac{N_{Ed}}{\chi_{\min}A_{eff}f_y/\gamma_M}\right)+\left(\frac{k_{LT}M_{y,Ed}}{\chi_{LT}W_{eff,y}f_y/\gamma_M}\right)+\left(\frac{k_zM_{z,Ed}}{W_{eff,z}f_y/\gamma_M}\right)$$
$$=(n_{Ed})+(m_{y,Ed})+(m_{z,Ed})\le 1 \tag{8}$$

in which χ is the reduction factor for buckling phenomena, A and W are the area and the section modulus, respectively, f_y is the material yielding strength and subscript *eff* indicates the use of the effective cross section properties, when different from the gross ones (in the following it has been assumed $A_{eff}=A$ and $W_{eff}=W$).

In Eq. (8) three different terms can be identified: the former (n_{Ed}) associated with the effect of the axial load, already discussed with reference to the column design, and the letters related to the bending moment contributions along the principal cross-section axes ($m_{y,Ed}$and $m_{z,Ed}$). Furthermore, as to the contribution due to bending moment along the principal major axis ($m_{y,Ed}$), which generally coincides with the down-aisle direction, the reduction factor for lateral-torsional buckling (χ_{LT}) can be determined via Eq. (6) by substituting the axial load relative slenderness ($\bar{\lambda}$) with the one for lateral-torsional buckling of beam ($\bar{\lambda}_{LT}$),which depends on the theoretical elastic critical moment for lateral-torsional buckling (M_{cr}), being defined as

$$\bar{\lambda}_{LT}=\sqrt{\frac{W_{eff,y}f_y}{M_{cr}}} \tag{9}$$

Term k_{LT} is defined as

$$k_{LT}=1-\frac{\mu_{LT}N_{Sd}}{\chi_zA_{eff}f_y}\le 1 \tag{10}$$

with μ_{LT}defined as

$$\mu_{LT}=0,15\cdot(\bar{\lambda}_z\beta_{M,\mathrm{LT}}-1)\le 0,9 \tag{11}$$

where $\bar{\lambda}_z$ is the slenderness ratio for flexural buckling and $\beta_{M,LT}$ is an equivalent uniform moment factor for lateral-torsional buckling, which, in case of bending moment with a linear variation between the critical points of the upright, is defined as

$$\beta_{M,\mathrm{LT}}=1,8-0,7\frac{M_{\min}}{M_{\max}} \tag{12}$$

where M_{min} and M_{max} indicate respectively the minimum and the maximum bending moment at the end of the element.

As to the contribution due to the bending moment along the principal minor axis $m_{z,Ed}$ (i.e. the bending moment acting on the cross-aisle direction), term k_z is expressed by Eq. (10) by using term χ_z instead of χ_{LT} and with the limitation $k_z\le 1.5$. Parameter μ_z is defined as:

$$\mu_z=\bar{\lambda}_z(2\beta_{M,z}-4)\le 0,9 \tag{13}$$

Equivalent uniform moment factor $\beta_{M,z}$ is defined in Eq. (12) considering the moment distribution in the z-plane (cross-aisle direction).

5.1. Numerical applications

Contents of part 1 of this two parts paper have already underlined [2] the fundamental importance associated with a correct assessment of the critical load N_{cr}, which can be evaluated via different approaches admitted by the Code, or not in contrast with this. In particular, it has been shown that the weak point of the code is the absence of univocal requirements for the evaluation of the effective length in the down-aisle direction, which directly influences in addition to the flexural critical load, also the flexural–torsional buckling load for mono-symmetric cross-section members. Owing to the importance of N_{cr} for the verification check of beam–column, due to the fact that n_{Ed} is the more influent term of

Eq. (8), the following alternatives deriving from the ones already discussed for the assessment critical buckling load or multiplier have been applied to evaluate the safety indices (*SI*), which are in the following identified as

Table 6
Dimensionless contribution due to the bi-moment on the cross-section resistance check.

$SI_G^{BM(7)}/SI_G^7$	$\rho_{j,btc}$	C.U.: $\rho_{j,base}$			E.U.: $\rho_{j,base}$		
		0.15	0.30	0.45	0.15	0.30	0.45
Racks M_4	0.5	0.015	0.029	0.028	0.022	0.021	0.020
	1.0	0.043	0.041	0.050	0.047	0.043	0.042
	1.5	0.044	0.058	0.057	0.064	0.059	0.069
	2.0	0.047	0.065	0.071	0.068	0.071	0.079
	3.5	0.051	0.075	0.084	0.082	0.088	0.092
	5.0	0.052	0.077	0.090	0.091	0.099	0.102
	7.0	0.049	0.081	0.091	0.094	0.105	0.105
	10.0	0.046	0.080	0.093	0.097	0.105	0.109
	mean	0.043	0.063	0.071	0.070	0.074	0.077
	max	0.052	0.081	0.093	0.097	0.105	0.109
Racks M_5	0.5	0.042	0.041	0.040	0.063	0.076	0.075
	1.0	0.058	0.063	0.062	0.122	0.126	0.123
	1.5	0.071	0.073	0.078	0.152	0.159	0.155
	2.0	0.077	0.088	0.087	0.177	0.179	0.182
	3.5	0.093	0.109	0.115	0.222	0.228	0.227
	5.0	0.100	0.121	0.128	0.244	0.254	0.253
	7.0	0.104	0.133	0.146	0.261	0.270	0.273
	10.0	0.105	0.142	0.159	0.275	0.289	0.291
	mean	0.081	0.096	0.102	0.190	0.198	0.198
	max	0.105	0.142	0.159	0.275	0.289	0.291
Racks T_3	0.5	0.000	0.016	0.016	0.000	0.000	0.000
	1.0	0.012	0.012	0.011	0.000	0.000	0.000
	1.5	0.010	0.019	0.019	0.016	0.014	0.014
	2.0	0.009	0.017	0.016	0.014	0.012	0.012
	3.5	0.015	0.021	0.027	0.011	0.020	0.019
	5.0	0.014	0.025	0.024	0.010	0.018	0.017
	7.0	0.013	0.023	0.028	0.010	0.017	0.016
	10.0	0.013	0.022	0.027	0.009	0.016	0.022
	mean	0.011	0.019	0.021	0.009	0.012	0.012
	max	0.015	0.025	0.028	0.016	0.020	0.022
Racks T_4	0.5	0.014	0.014	0.014	0.000	0.000	0.000
	1.0	0.010	0.019	0.019	0.016	0.015	0.015
	1.5	0.017	0.016	0.023	0.013	0.012	0.012
	2.0	0.015	0.021	0.020	0.011	0.021	0.020
	3.5	0.018	0.022	0.026	0.018	0.016	0.024
	5.0	0.021	0.024	0.028	0.016	0.021	0.021
	7.0	0.019	0.026	0.030	0.015	0.019	0.025
	10.0	0.018	0.028	0.031	0.014	0.024	0.023
	mean	0.016	0.021	0.024	0.013	0.016	0.017
	max	0.021	0.028	0.031	0.018	0.024	0.025

- SI_{BC}^{SL+FT}: the safety index associated with the values of the appropriate system length for the flexural, torsional and flexural–torsional buckling loads. In case of bi-symmetric cross-section members, it is indicated as SI_{BC}^{SL}, owing to the absence of flexural–torsional instability;
- SI_{BC}^{W+FT}: the safety index associated with the flexural buckling in the down-aisle direction considered via the modified Wood's approach, i.e. [18], in accordance with the criteria proposed by ECCS [19]. In case of bi-symmetric cross-section members, it is indicated as SI_{BC}^{W}, owing to the absence of flexural–torsional instability;
- SI_{BC}^{6+FT}: the safety index related to a buckling analysis via 6DOFs FE beam element formulation combined with the evaluation of flexural–torsional buckling load multiplier of a suitable isolated member (hybrid procedure). In case of bi-symmetric cross-section members, it is indicated as SI_{BC}^{6}, owing to the absence of flexural–torsional instability; and
- SI_{BC}^{7}: the safety index related to a buckling analysis via 7DOFs FE formulations, which allow to evaluate directly the elastic critical load N_{cr}. In case of bi-symmetric cross-section members, it is indicated as SI_{BC}^{7}, and it is expected to be practically coincident with index SI_{BC}^{6}, owing to the extremely limited influence of the flexural moment in the geometric stiffness matrix, as discussed in the previous part of this paper.

As to the material, S350 steel grade [20] was considered for uprights, which represents the most commonly used steel grade class for storage pallet racks.

In order to allow a better appraisal of the research results, main data related to SI_{BC} are presented by separating the cases of bi-symmetric (L_racks) and mono-symmetric cross-section (M_ and T_ racks) uprights.

With reference to the L_racks, the application of the three discussed design alternatives leads to evaluate SI_{BC}^{SL}, SI_{BC}^{W} and SI_{BC}^{6} and the ratios SI_{BC}^{6}/SI_{BC}^{SL} and SI_{BC}^{6}/SI_{BC}^{W} are presented in Tables 7 and 8, respectively. It can be noted that the use of the system length approach is absolutely inadequate for design purposes: for the lowest values of the beam-to-column joint stiffness the load carrying capacity is significantly over-estimated, up to more than 2 times (up to 2.7). Increasing $\rho_{j,btc}$, ratio SI_{BC}^{6}/SI_{BC}^{SL} decreases significantly but in any case it is much greater than 1, never lower than 1.03, with a mean value approximately equal to 1.55 for C.U. and 1.40 for E.U. In Fig. 19 the ratio SI_{BC}^{6}/SI_{BC}^{W} is plotted versus $\rho_{j,btc}$ and the frequency and cumulated relative frequency distribution are presented in Fig. 20: several data are in the range 1.4–1.9 and the 95% fractile value is approximately 2.10. Overestimation of the actual safety index is significantly reduced by the use of Wood's approach for semi-continuous frames, As it appears from Table 8,

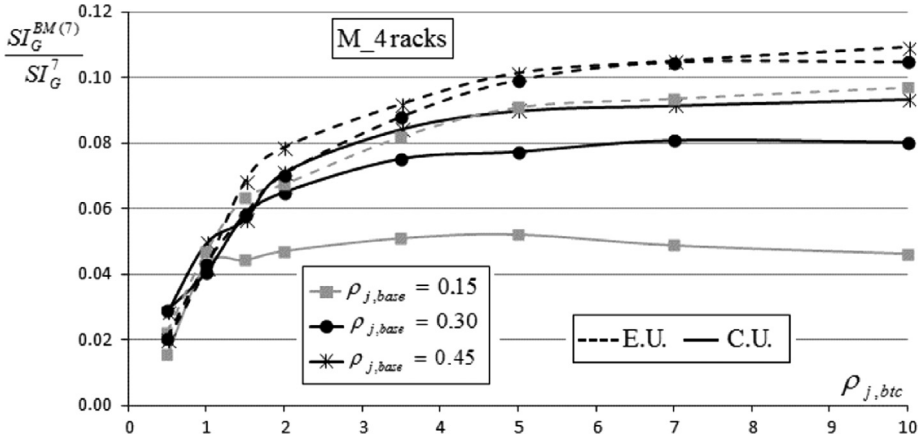

Fig. 14. $SI_G^{BM(7)}/SI_G^7 - \rho_{j,btc}$ relationships for M_4 racks.

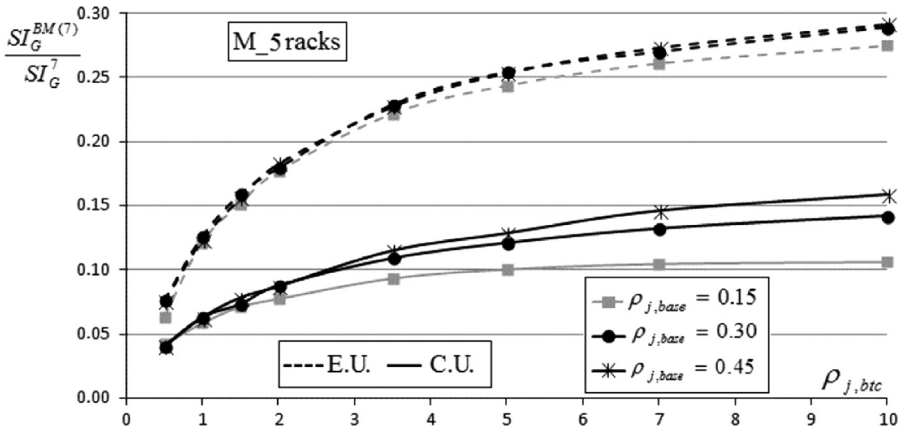

Fig. 15. $SI_G^{BM(7)}/SI_G^7 - \rho_{j,btc}$ relationships for M_5 racks.

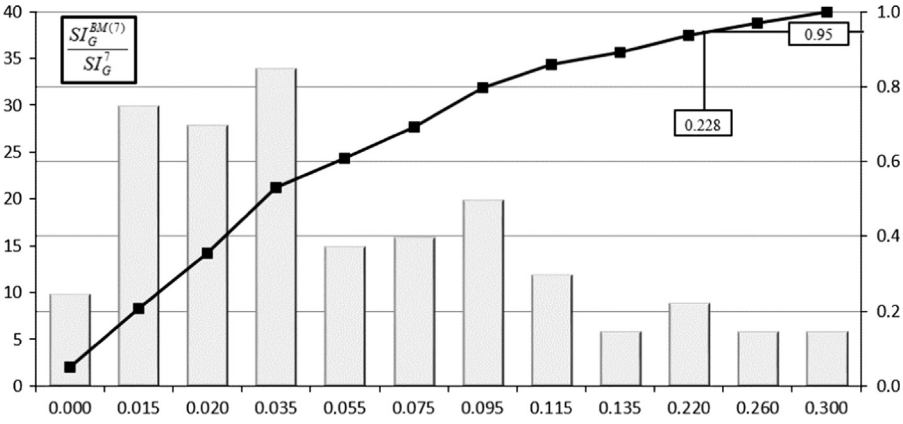

Fig. 16. Frequency and cumulated relative frequency of ratio $SI_G^{BM(7)}/SI_G^7$ for M_ and T_ racks, for the more stressed central upright.

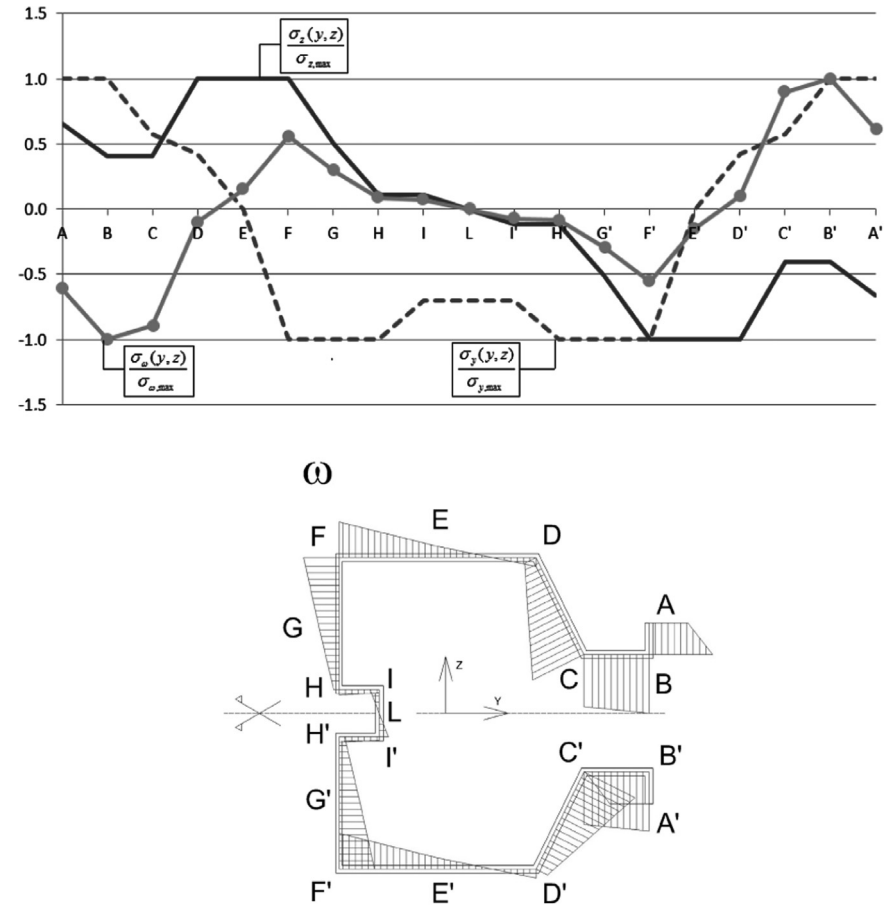

Fig. 17. Distribution along the M_cross-section perimeter of $\sigma_y(y,z)/\sigma_{y,\max}$, $\sigma_z(y,z)/\sigma_{z,\max}$ and $\sigma_\omega(y,z)/\sigma_{\omega,\max}$.

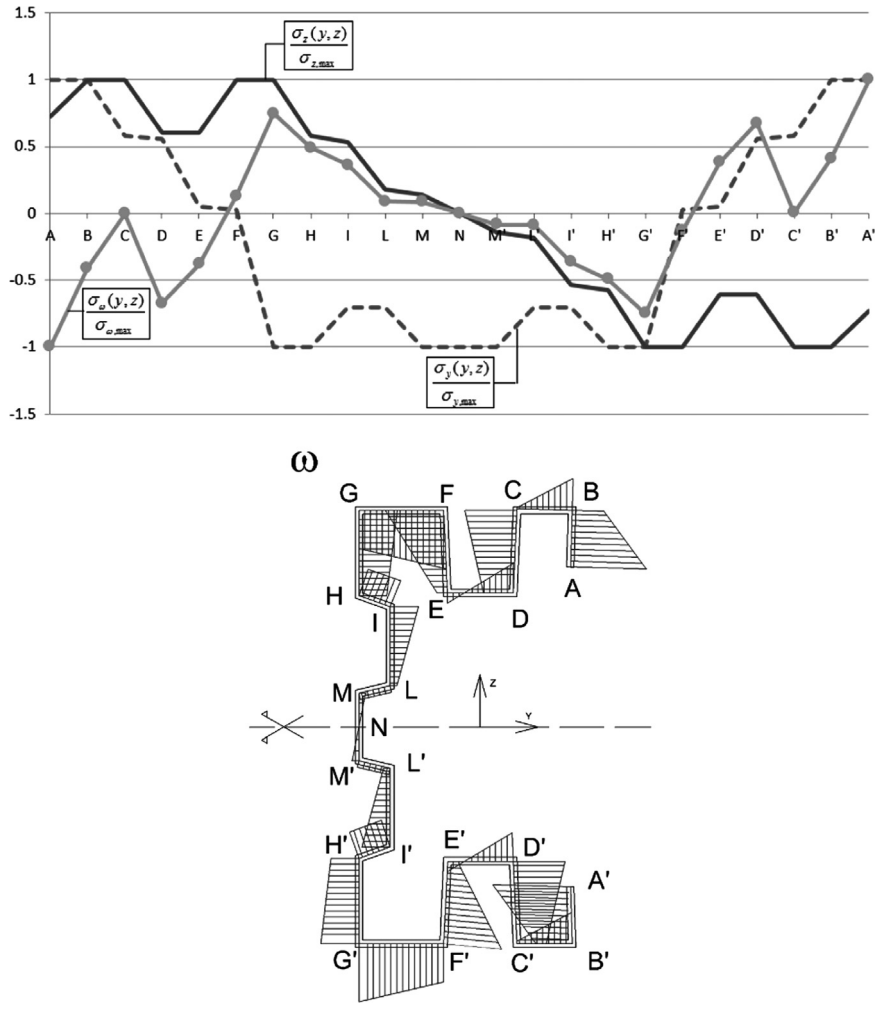

Fig. 18. Distribution along the T_cross-section perimeter of $\sigma_y(y,z)/\sigma_{y,\,max}$, $\sigma_z(y,z)/\sigma_{z,\,max}$ and $\sigma_\omega(y,z)/\sigma_{\omega,\,max}$.

Table 7
Accuracy of the system length approach for racks with bi-symmetric uprights.

SI^6_{BC}/SI^{SL}_{BC}	$\rho_{j,btc}$	C.U.: $\rho_{j,base}$			E.U.: $\rho_{j,base}$		
		0.15	0.30	0.45	0.15	0.30	0.45
Racks L_3	0.5	2.635	2.505	2.471	2.268	2.142	2.108
	1.0	2.037	1.951	1.919	1.802	1.721	1.692
	1.5	1.763	1.690	1.659	1.579	1.514	1.492
	2.0	1.608	1.540	1.517	1.461	1.395	1.370
	3.5	1.388	1.323	1.305	1.255	1.221	1.205
	5.0	1.288	1.232	1.212	1.163	1.129	1.119
	7.0	1.226	1.166	1.146	1.103	1.075	1.064
	10.0	1.174	1.118	1.100	1.064	1.035	1.027
	mean	1.640	1.565	1.541	1.462	1.404	1.385
	max	2.635	2.505	2.471	2.268	2.142	2.108
Racks L_5	0.5	2.438	2.391	2.367	2.123	2.082	2.056
	1.0	1.877	1.832	1.824	1.692	1.650	1.638
	1.5	1.632	1.594	1.584	1.495	1.465	1.449
	2.0	1.493	1.463	1.452	1.387	1.357	1.345
	3.5	1.298	1.275	1.267	1.226	1.199	1.190
	5.0	1.212	1.192	1.187	1.152	1.136	1.129
	7.0	1.158	1.137	1.133	1.096	1.083	1.085
	10.0	1.115	1.098	1.092	1.060	1.047	1.044
	mean	1.528	1.498	1.488	1.404	1.377	1.367
	max	2.438	2.391	2.367	2.123	2.082	2.056

Table 8
Accuracy of the modified Wood's approach for racks with bi-symmetric uprights

SI^6_{BC}/SI^{W}_{BC}	$\rho_{j,btc}$	C.U.: $\rho_{j,base}$			E.U.: $\rho_{j,base}$		
		0.15	0.30	0.45	0.15	0.30	0.45
Racks L_3	0.5	1.456	1.439	1.438	1.396	1.369	1.363
	1.0	1.228	1.218	1.214	1.191	1.177	1.172
	1.5	1.132	1.122	1.114	1.101	1.092	1.089
	2.0	1.081	1.069	1.064	1.061	1.046	1.039
	3.5	1.015	0.996	0.993	0.991	0.983	0.980
	5.0	0.985	0.969	0.962	0.965	0.952	0.949
	7.0	0.971	0.949	0.941	0.946	0.937	0.932
	10.0	0.958	0.936	0.929	0.936	0.925	0.923
	mean	1.103	1.087	1.082	1.073	1.060	1.056
	max	1.456	1.439	1.438	1.396	1.369	1.363
Racks L_5	0.5	1.767	1.778	1.774	1.640	1.645	1.636
	1.0	1.420	1.418	1.422	1.349	1.343	1.343
	1.5	1.275	1.271	1.272	1.223	1.222	1.217
	2.0	1.195	1.194	1.193	1.157	1.153	1.150
	3.5	1.088	1.086	1.086	1.063	1.057	1.055
	5.0	1.042	1.040	1.041	1.022	1.022	1.021
	7.0	1.015	1.011	1.012	0.995	0.991	0.995
	10.0	0.994	0.992	0.991	0.979	0.974	0.974
	mean	1.224	1.224	1.224	1.179	1.176	1.174
	max	1.767	1.778	1.774	1.640	1.645	1.636

ratio SI^6_{BC}/SI^W_{BC} is never greater than 1.46 and 1.78 for L_3 and L_5 racks. respectively. For $\rho_{j,btc}, \geq 3$ it is slightly lower than unity (up to 0.92): mean value for C.U is 1.16. and for E.U. is 1.12. In Fig. 21 the ratio SI^6_{BC}/SI^W_{BC} is plotted versus $\rho_{j,btc}$. and the frequency and cumulated relative frequency distribution are presented in Fig. 22. In general, it can be noted that the overestimation of the safety

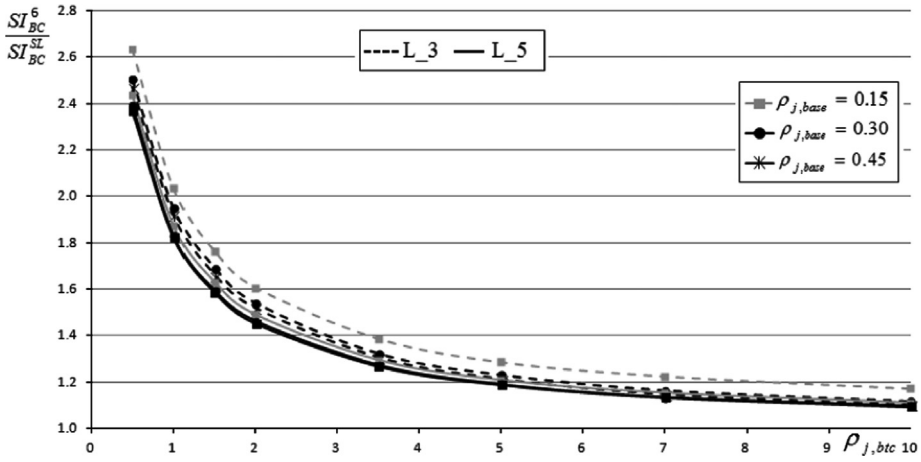

Fig. 19. $SI_{BC}^{7}/SI_{BC}^{SL} - \rho_{j,btc}$ relationships for L_3 and L_5 racks (data related to the more stressed internal upright).

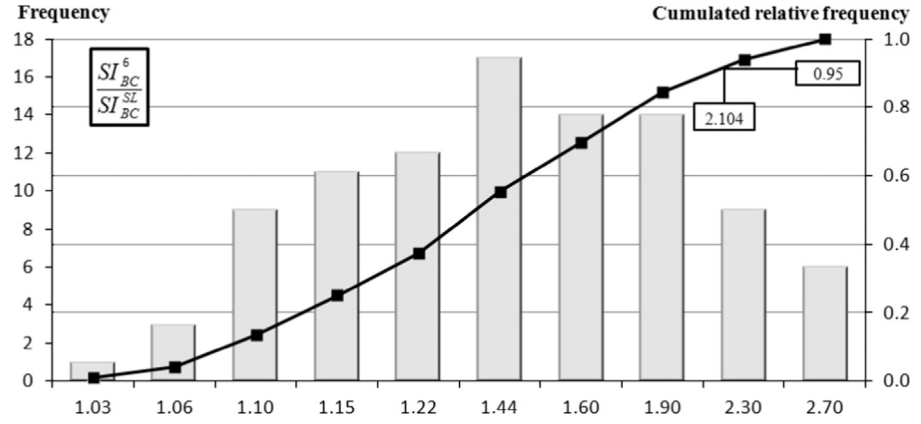

Fig. 20. Frequency and cumulated relative frequency of ratio SI_{BC}^{7}/SI_{BC}^{SL} for L_racks, for the more stressed central upright.

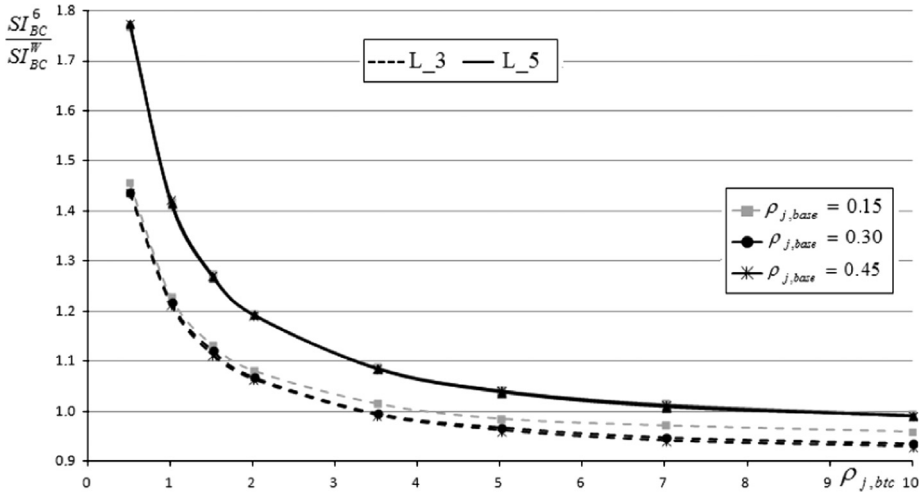

Fig. 21. $SI_{BC}^{7}/SI_{BC}^{W} - \rho_{j,btc}$ relationships for L_3 and L_5 racks (data related to the more stressed internal upright).

index SI_{BC}^{6} is significantly reduced by the use of this second approach, despite the fact that with reference to the frequency, many data are in the range 1.0–1.45. The presence of several data for greater values of the ratio SI_{BC}^{6}/SI_{BC}^{W} contributes to determine a 95% fractile value quite high, approximately equal to 2.0.

If reference is made to racks with mono-symmetric cross-section uprights, safety indices associated with the considered design approaches are SI_{BC}^{SL+FT}, SI_{BC}^{W+FT}, SI_{BC}^{6+FT} and SI_{BC}^{7}: it is assumed that SI_{BC}^{7} represents the most accurate evaluation of the safety index and hence the ratios $SI_{BC}^{7}/SI_{BC}^{SL+FT}$, $SI_{BC}^{7}/SI_{BC}^{W+FT}$ and $SI_{BC}^{7}/SI_{BC}^{6+FT}$ allow a direct appraisal of the accuracy of these design alternatives. From the data in Table 9, where the dimensionless data related to the system length approach accuracy (i.e. $SI_{BC}^{7}/SI_{BC}^{SL+FT}$) are presented, it can be noted that the required flexural–torsional buckling check on isolated uprights reduces remarkably the overestimation of the safety of the racks.; if a comparison is made with the corresponding results obtained for L_racks. For M_racks, the ratio $SI_{BC}^{7}/SI_{BC}^{SL+FT}$ ranges from C.U.

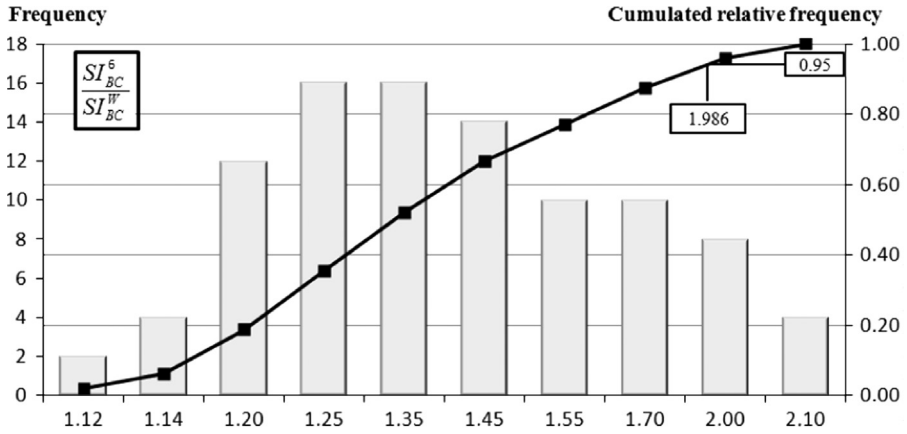

Fig. 22. Frequency and cumulated relative frequency of ratio SI_{BC}^{7}/SI_{BC}^{W} for L_racks, for the more stressed central upright.

Table 9
Accuracy of the system length approach for racks with mono-symmetric uprights.

$SI_{BC}^{7}/SI_{BC}^{SL+FT}$	$\rho_{j,btc}$	C.U.: $\rho_{j,base}$			E.U.: $\rho_{j,base}$		
		0.15	0.30	0.45	0.15	0.30	0.45
Racks M_4	0.5	2.228	2.145	2.100	2.233	2.148	2.115
	1.0	1.725	1.666	1.647	1.732	1.677	1.658
	1.5	1.535	1.474	1.461	1.469	1.444	1.432
	2.0	1.442	1.379	1.356	1.321	1.305	1.301
	3.5	1.325	1.264	1.246	1.178	1.124	1.126
	5.0	1.271	1.221	1.202	1.137	1.083	1.063
	7.0	1.235	1.189	1.170	1.110	1.060	1.040
	10.0	1.212	1.159	1.151	1.092	1.042	1.025
	mean	1.497	1.437	1.417	1.409	1.360	1.345
	max	2.228	2.145	2.100	2.233	2.148	2.115
Racks M_5	0.5	1.686	1.654	1.637	1.547	1.512	1.497
	1.0	1.366	1.344	1.330	1.298	1.270	1.261
	1.5	1.243	1.226	1.214	1.182	1.165	1.159
	2.0	1.179	1.159	1.156	1.079	1.072	1.073
	3.5	1.093	1.081	1.076	0.974	0.962	0.959
	5.0	1.060	1.049	1.043	0.930	0.926	0.924
	7.0	1.037	1.026	1.023	0.913	0.896	0.897
	10.0	1.017	1.008	1.006	0.901	0.876	0.876
	mean	1.210	1.193	1.186	1.103	1.085	1.081
	max	1.686	1.654	1.637	1.547	1.512	1.497
Racks T_3	0.5	2.070	2.009	1.986	2.070	2.009	1.986
	1.0	1.695	1.619	1.599	1.694	1.619	1.599
	1.5	1.541	1.478	1.465	1.540	1.478	1.465
	2.0	1.455	1.404	1.385	1.456	1.403	1.385
	3.5	1.354	1.302	1.284	1.354	1.301	1.284
	5.0	1.310	1.256	1.245	1.311	1.256	1.245
	7.0	1.293	1.234	1.218	1.294	1.235	1.221
	10.0	1.272	1.218	1.203	1.271	1.217	1.203
	mean	1.499	1.440	1.423	1.499	1.440	1.424
	max	2.070	2.009	1.986	2.070	2.009	1.986
Racks T_4	0.5	1.986	1.933	1.909	1.985	1.932	1.909
	1.0	1.595	1.556	1.542	1.594	1.555	1.541
	1.5	1.438	1.406	1.392	1.438	1.406	1.392
	2.0	1.356	1.324	1.315	1.355	1.324	1.314
	3.5	1.239	1.212	1.206	1.238	1.212	1.205
	5.0	1.195	1.168	1.161	1.195	1.168	1.160
	7.0	1.166	1.140	1.138	1.171	1.144	1.137
	10.0	1.145	1.122	1.114	1.149	1.122	1.113
	mean	1.390	1.358	1.347	1.391	1.358	1.346
	max	1.986	1.933	1.909	1.985	1.932	1.909

between 1.11 and 2.23 while. for T_racks, the minimum and maximum values are 1.11 and 2.07, respectively. Also for this 1st approach. the ratio is slightly greater for C.U. than for E.U. and the values decrease with the increase of the joint stiffness (both beam-to-column and base plate connections). Figs. 23 and 24 represent. for the more stressed C.U., the curve $SI_{BC}^{7}/SI_{BC}^{SL+FT} - \rho_{j,btc}$ for the

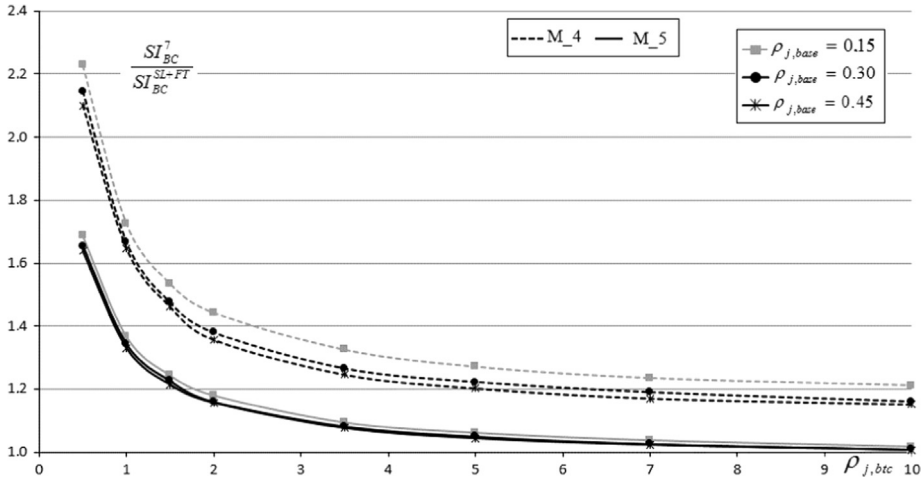

Fig. 23. $SI_{BC}^{7}/SI_{BC}^{SL+FT} - \rho_{j,btc}$ relationships for M_4 and M_5 racks (data related to the more stressed internal upright).

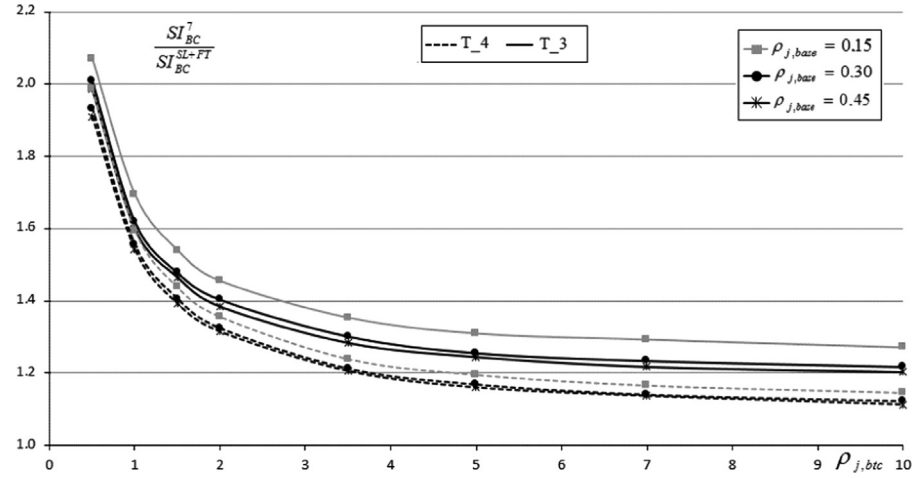

Fig. 24. $SI_{BC}^{7}/SI_{BC}^{SL+FT} - \rho_{j,btc}$ relationships for T_3 and T_4 racks (data related to the more stressed internal upright).

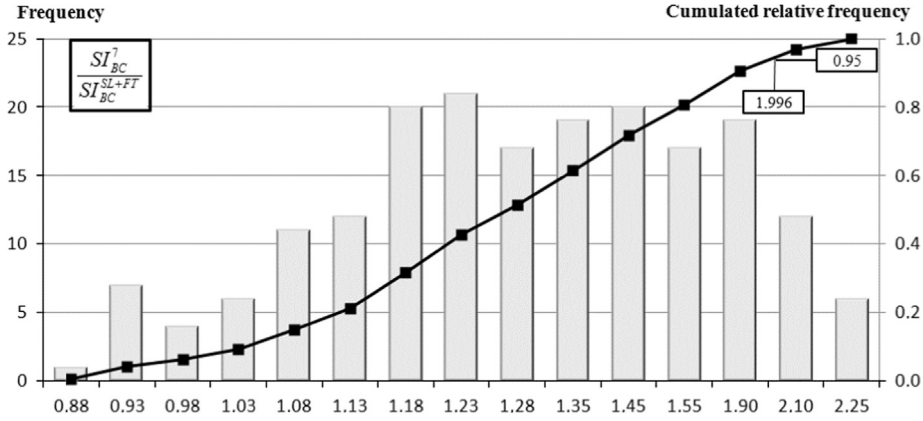

Fig. 25. Frequency and cumulated relative frequency of ratio $SI_{BC}^{7}/SI_{BC}^{SL+FT}$ for M_and T_racks, for the more stressed central upright.

M_ and T_racks. respectively. while in Fig. 25 the relative and cumulated frequency are plotted with the 95% fractile value (approximately equal to 2.0) in evidence.

The accuracy of the modified Wood's approach is summarized by the data in Table 10. where the ratio $SI_{BC}^{7}/SI_{BC}^{W+FT}$ is presented. It can be noted that all the values are greater than unity: also in this case the error decreases with the increase of the joint stiffness but the level of overestimation of the safety index is significantly reduced, not greater than 32% with the exception of 44% for T_4 racks. Figs. 26 and 27 present the curve $SI_{BC}^{7}/SI_{BC}^{W+FT} - \rho_{j,btc}$ for the internal uprights of M_ and T_racks respectively, while in Fig. 28 the frequency and cumulated relative frequency are plotted with the 95% fractile value (approximately equal to 1.3).

The combined (hybrid) approach (6DOFs FE buckling analysis combined with the flexural–torsional buckling checks on isolated members) seems to be the most suitable for design purposes,

Table 10
Accuracy of the modified Wood's approach for racks with mono-symmetric uprights.

$SI_{BC}^{7}/SI_{BC}^{W+FT}$	$\rho_{j,btc}$	C.U.: $\rho_{j,base}$			E.U.: $\rho_{j,base}$		
		0.15	0.30	0.45	0.15	0.30	0.45
Racks M_4	0.5	1.250	1.251	1.241	1.321	1.322	1.320
	1.0	1.084	1.084	1.084	1.146	1.146	1.148
	1.5	1.033	1.024	1.027	1.057	1.066	1.066
	2.0	1.017	1.002	0.996	1.002	1.013	1.018
	3.5	1.009	0.989	0.984	0.968	0.942	0.949
	5.0	1.006	0.992	0.985	0.968	0.939	0.927
	7.0	1.007	0.992	0.985	0.969	0.941	0.929
	10.0	1.012	0.990	0.991	0.972	0.942	0.932
	mean	1.052	1.040	1.037	1.050	1.039	1.036
	max	1.250	1.251	1.241	1.321	1.322	1.320
Racks M_5	0.5	1.246	1.250	1.247	1.208	1.206	1.202
	1.0	1.065	1.068	1.065	1.058	1.055	1.055
	1.5	1.004	1.008	1.004	0.996	0.998	0.998
	2.0	0.976	0.975	0.978	0.934	0.941	0.947
	3.5	0.944	0.947	0.947	0.880	0.880	0.880
	5.0	0.936	0.938	0.937	0.858	0.862	0.863
	7.0	0.931	0.932	0.933	0.854	0.845	0.849
	10.0	0.926	0.927	0.930	0.852	0.835	0.837
	mean	1.003	1.006	1.005	0.955	0.953	0.954
	max	1.246	1.250	1.247	1.208	1.206	1.202
Racks T_3	0.5	1.300	1.303	1.301	1.299	1.303	1.301
	1.0	1.155	1.134	1.131	1.154	1.134	1.131
	1.5	1.109	1.093	1.092	1.109	1.093	1.091
	2.0	1.089	1.077	1.071	1.090	1.076	1.071
	3.5	1.082	1.064	1.058	1.083	1.064	1.058
	5.0	1.084	1.062	1.059	1.084	1.061	1.059
	7.0	1.098	1.069	1.062	1.098	1.070	1.064
	10.0	1.103	1.077	1.071	1.103	1.077	1.071
	mean	1.127	1.110	1.105	1.128	1.110	1.106
	max	1.300	1.303	1.301	1.299	1.303	1.301
Racks T_4	0.5	1.438	1.436	1.430	1.438	1.435	1.430
	1.0	1.224	1.220	1.218	1.223	1.219	1.217
	1.5	1.147	1.144	1.140	1.147	1.144	1.140
	2.0	1.111	1.105	1.104	1.111	1.105	1.104
	3.5	1.065	1.059	1.059	1.065	1.058	1.058
	5.0	1.053	1.044	1.042	1.053	1.044	1.042
	7.0	1.046	1.037	1.039	1.051	1.040	1.038
	10.0	1.044	1.035	1.031	1.047	1.035	1.031
	mean	1.141	1.135	1.133	1.142	1.135	1.133
	max	1.438	1.436	1.430	1.438	1.435	1.430

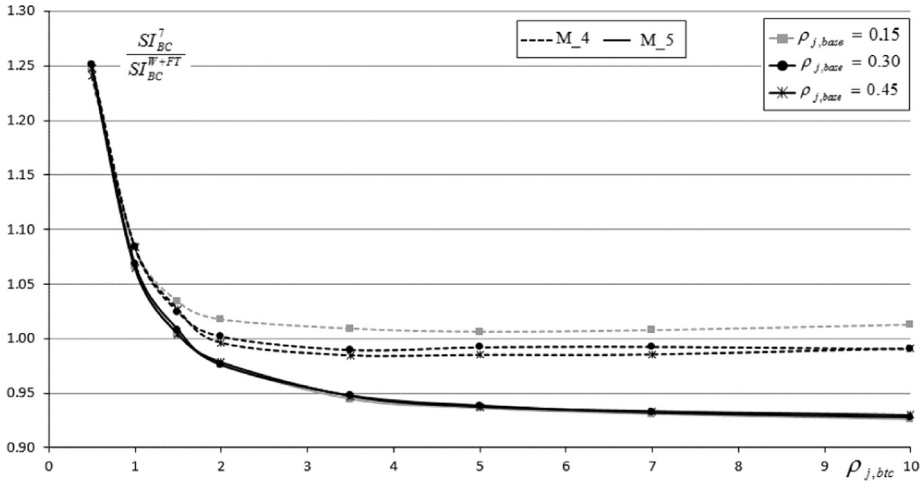

Fig. 26. $SI_{BC}^{7}/SI_{BC}^{W+FT} - \rho_{j,btc}$ relationships for M_4 and M_5 racks (data related to the more stressed internal upright).

as it appears from Table 11 where the ratio $SI_{BC}^{7}/SI_{BC}^{6+FT}$ is presented. The safety index is slightly overestimated but the errors are quite limited, never greater than 10%, except for T_3 racks, for which the safety index is underestimated up to 15% with reference to external uprights. Figs. 29 and 30 represent the curve $SI_{BC}^{7}/SI_{BC}^{6+FT} - \rho_{j,btc}$ for the M_ and T_racks respectively, while in Fig. 31 the frequency and cumulated relative frequency are plotted with the 95% fractile value (approximately equal to 1.13).

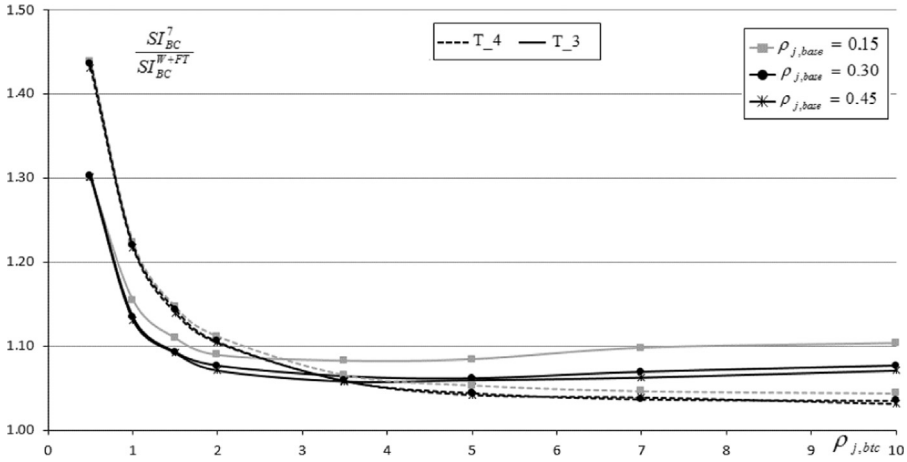

Fig. 27. $SI_{BC}^{7}/SI_{BC}^{W+FT} - \rho_{j,btc}$ relationships for T_3 and T_4 racks (data related to the more stressed internal upright).

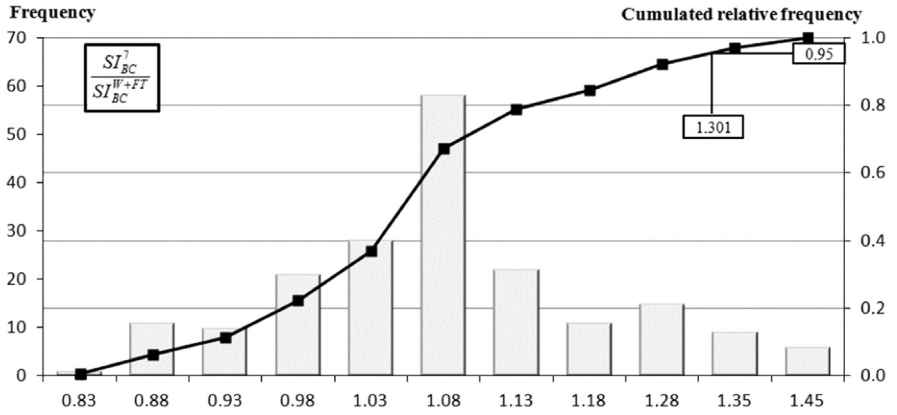

Fig. 28. Relative and cumulated frequency of ratio $SI_{BC}^{7}/SI_{BC}^{W+FT}$ for M_and T_racks, for the more stressed central upright.

It should be noted that these results underline that warping effects are of paramount importance for a safe rack design and the differences in the load carrying capacity associated with the different approaches are absolutely non negligible in terms of structural safety as well as optimal use of the materials.

Finally, it worth to mention that the behavior of M_4 racks is significantly influenced by the coupling between flexure and torsion. In particular, as already noted in Ref [21], bending moments in the down-aisle direction depend on the adopted FE beam formulation. Neglecting warping, lower values of the bending moments govern verification checks: for this reason the ratio between the safety index reported in Tables 4 and 5 is significantly different from the ones associated with the other racks, which are characterized by a reduced value of the inter-story height and/or higher values of the joint rotational stiffness.

6. Conclusions

A two-parts paper has been proposed to summarize the preliminary outcomes of a research project on the design rules currently adopted in Europe. In the companion paper [2] attention has been paid on the method of analysis for the evaluation of the design internal forces and moments: the different alternatives directly admitted by the code, or not in contrast with it, have been considered by demonstrating that they can lead to results significantly different from each other. Verification checks have been discussed in this second part of the paper considering the serviceability limit state associated with lateral rack displacements as well as the ultimate limit states of both resistance and stability for uprights. Influence of warping has been appraised via the comparison of FE analysis results of a traditional 6DOFs beam formulation and a more refined one to which the 7th DOF (warping of the cross-section) has been added to consider adequately warping effects (Wagner's constant, warping torsion, shear center eccentricity and the coupling between bending and torsion). On the basis of the 144 modeled racks, it can be concluded that when mono-symmetric cross section uprights are used, the influence of warping cannot be absolutely neglected and the verification checks for serviceability and ultimate limit states are significantly influenced by the set of displacement and internal forces and bending moments obtained from the structural analysis. Furthermore, neglecting warping leads to overestimating the lateral displacement significantly, up to 37%. Great differences have been observed also in the values of the bending moments along both the down- and the cross-aisle direction, which contribute to different values of the safety index. Cross-section performance is significantly influenced by the contribution of bi-moment, which also increases also significantly the safety index associated with the verification checks, approximately up to 1.4 times.

The design alternatives for beam–column uprights have been applied and the associated results have been compared in terms of safety index, which differ mainly for the approach adopted to

Table 11
Accuracy of the hybrid procedure (buckling 6DOFs FE analysis combined with flexural–torsional check on isolated member).

$SI_{BC}^{7}/SI_{BC}^{6+FT}$	$\rho_{j,btc}$	C.U.: $\rho_{j,base}$			E.U.: $\rho_{j,base}$		
		0.15	0.30	0.45	0.15	0.30	0.45
Racks M_4	0.5	1.011	1.016	1.018	1.092	1.103	1.099
	1.0	1.015	1.018	1.023	1.083	1.088	1.096
	1.5	1.018	1.021	1.025	1.055	1.070	1.071
	2.0	1.021	1.025	1.026	1.024	1.042	1.051
	3.5	1.043	1.044	1.045	1.010	0.995	1.007
	5.0	1.048	1.053	1.057	1.014	0.998	0.990
	7.0	1.051	1.059	1.062	1.014	1.001	0.993
	10.0	1.057	1.061	1.069	1.017	1.002	0.995
	mean	1.035	1.038	1.039	1.039	1.037	1.038
	max	1.057	1.062	1.069	1.092	1.103	1.099
Racks M_5	0.5	0.934	0.937	0.933	0.946	0.947	0.944
	1.0	0.932	0.933	0.931	0.951	0.949	0.950
	1.5	0.933	0.938	0.935	0.947	0.951	0.952
	2.0	0.937	0.938	0.941	0.917	0.927	0.933
	3.5	0.942	0.948	0.948	0.891	0.894	0.896
	5.0	0.945	0.952	0.952	0.876	0.884	0.886
	7.0	0.943	0.952	0.955	0.875	0.870	0.875
	10.0	0.940	0.951	0.955	0.873	0.860	0.863
	mean	0.938	0.944	0.944	0.909	0.910	0.912
	max	0.945	0.952	0.955	0.951	0.951	0.952
Racks T_3	0.5	1.058	1.072	1.069	1.058	1.072	1.069
	1.0	1.087	1.091	1.093	1.087	1.091	1.093
	1.5	1.096	1.103	1.108	1.095	1.103	1.108
	2.0	1.105	1.113	1.115	1.106	1.115	1.116
	3.5	1.121	1.123	1.124	1.121	1.128	1.125
	5.0	1.119	1.124	1.132	1.119	1.121	1.132
	7.0	1.128	1.129	1.133	1.132	1.130	1.134
	10.0	1.129	1.131	1.134	1.129	1.131	1.135
	mean	1.106	1.111	1.113	1.106	1.111	1.114
	max	1.132	1.131	1.134	1.132	1.131	1.135
Racks T_4	0.5	1.015	1.017	1.015	1.015	1.017	1.014
	1.0	1.016	1.014	1.013	1.016	1.014	1.012
	1.5	1.013	1.015	1.012	1.013	1.015	1.013
	2.0	1.015	1.015	1.016	1.014	1.015	1.016
	3.5	1.015	1.018	1.020	1.015	1.017	1.019
	5.0	1.019	1.022	1.022	1.019	1.021	1.022
	7.0	1.021	1.026	1.032	1.026	1.029	1.031
	10.0	1.024	1.032	1.033	1.028	1.032	1.032
	mean	1.017	1.020	1.020	1.018	1.020	1.020
	max	1.024	1.032	1.033	1.028	1.032	1.032

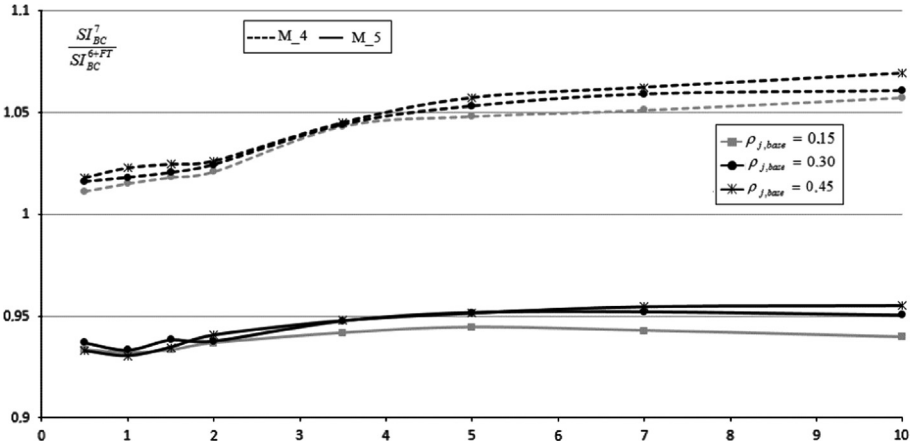

Fig. 29. $SI_{BC}^{7}/SI_{BC}^{6+FT}-\rho_{j,btc}$ relationships for M_4 and M_5 racks (data related to the more stressed internal upright).

evaluate the elastic critical load. The admitted possibilities, which serve also to evaluate the method of analysis, lead to results significantly different in terms of safety index. In case of bi-symmetric cross-section members, the system length or the FE buckling multiplier approaches lead to differences in the safety index up to 2.6. i.e. the 1st design approach (system length) leads to structures less expensive (but also less safe) than the racks designed via other approaches. As it can be noted from Fig. 32,

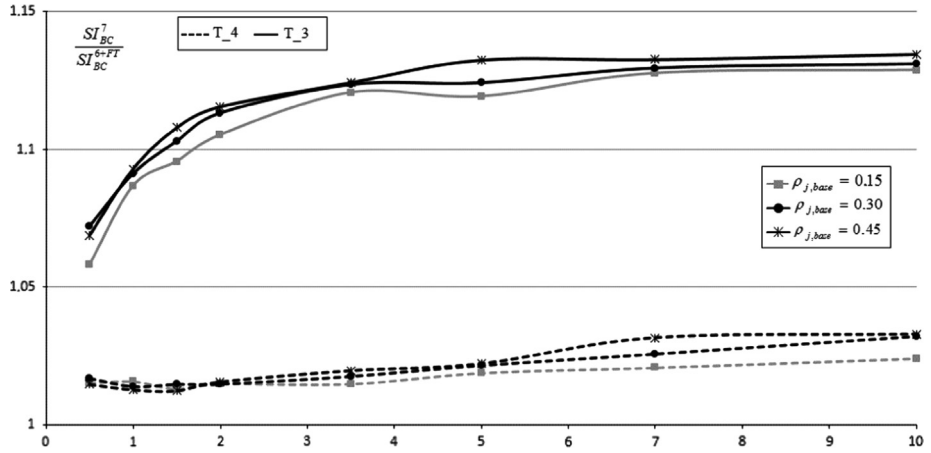

Fig. 30. $SI_{BC}^{7}/SI_{BC}^{6+FT}-\rho_{j,btc}$ relationships for T_3 and T_4 racks (data related to the more stressed internal upright).

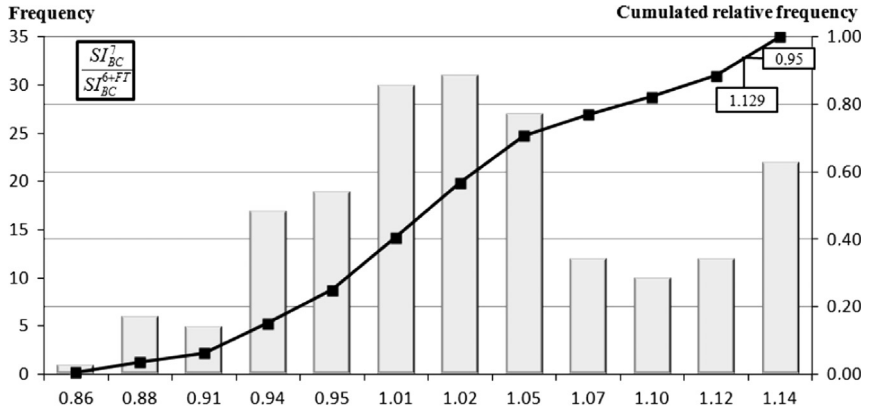

Fig. 31. Frequency and cumulated relative frequency of ratio $SI_{BC}^{7}/SI_{BC}^{6+FT}$ for M_ and T_ racks, for the more stressed central upright.

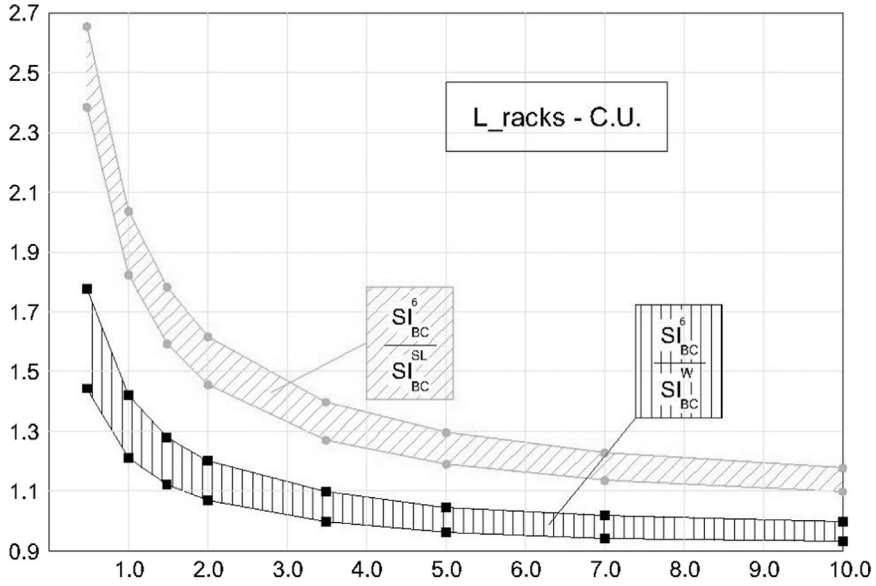

Fig. 32. Domain of errors committed with the use of the safety index obtained with Wood's method or with the system length, for the L_ racks.

which represents the domains associated with the two considered approaches, a significant reduction of the differences respect to the correct safety index (SI_{BC}^{6}) associated with the use of the overall buckling analysis multiplier is guaranteed by use of the 2nd approach, suitably modified to account for the presence of semi-continuous racks. These differences are however more limited in case of racks with mono-symmetric cross-section upright, owing to the additional check required for flexural–torsional buckling, Fig. 33 corresponds to Fig. 32 for racks with mono-symmetric cross section uprights: the width of the domains

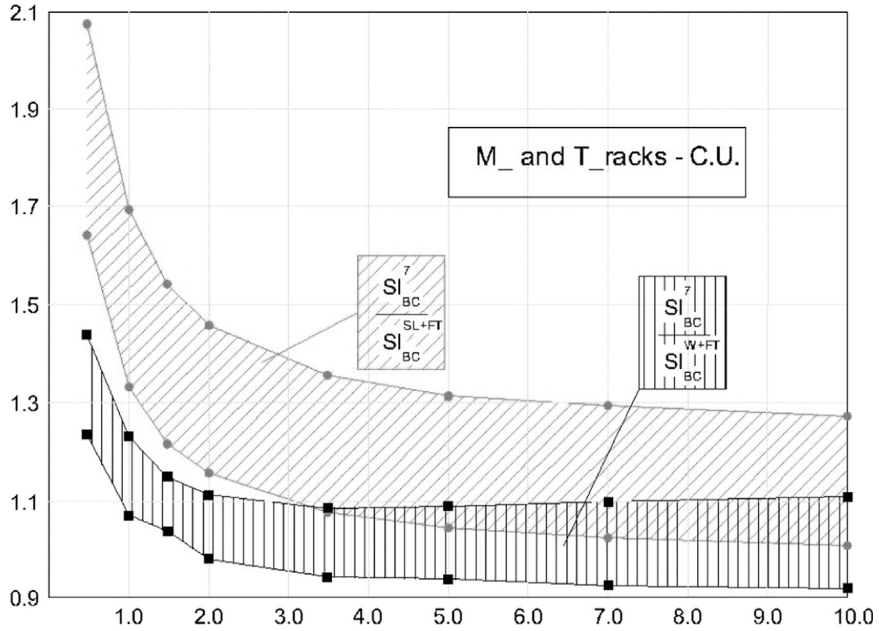

Fig. 33. Domain of errors committed with the use of the safety index obtained with Wood's method or with the system length, for the M_ and T_ racks.

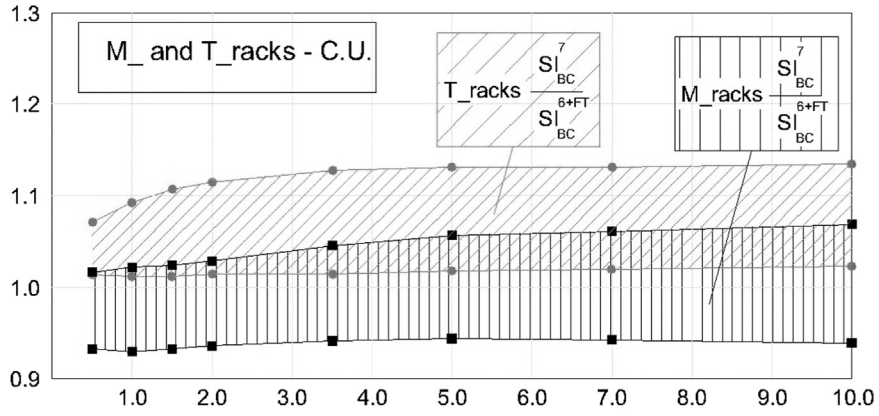

Fig. 34. Domain of errors committed with the use of the safety index obtained with the hybrid method, for the M_ and T_ racks.

associated with the three applied approaches is significantly reduced for the presence of the flexural–buckling checks and, in several cases, Wood's approach is slightly on the safe side. Moreover, it can be concluded that the sole approach appearing adequate for design purposes is the hybrid one, which is generally on the safe side leading to a non-excessive overestimation of the load carrying capacity (Fig. 34).

Finally, as a general conclusion, two further improvements are urgently required for the European rack design code: a univocal approach for the evaluation of the flexural buckling length and the definition of a set of minimum requirements for the adequacy of the FE analysis programs.

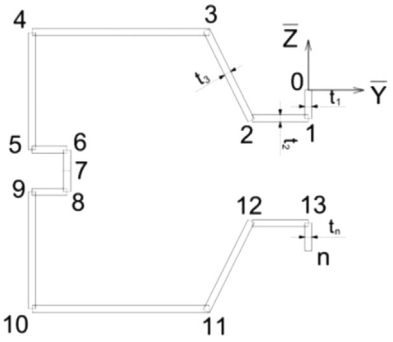

Fig. A1. Cross-section nodes.

Appendix A. Main cross-section geometrical parameters

A simplified procedure is proposed, which requires to divide the cross-section into n straight parts, each of them identified with a progressive number (from 1 to n). Nodes define each part, which are numbered progressively from 0 to n (the generic i-part is delimited by nodes $i-1$ and i). The location of each node can be identified in the reference system $\overline{y}-\overline{z}$ and each part of the cross-section has a constant effective thickness (t_i), as shown in Fig. A1.

The following parameters are of interest for practical design proposes.

- Sum of the area of cross-section parts, i.e. area of the cross-section:

$$A=\sum_{i=1}^{N} dA_i=\sum_{i=1}^{N} t_i\sqrt{(\overline{y}_i-\overline{y}_{i-1})^2+(\overline{z}_i-\overline{z}_{i-1})^2} \tag{A1}$$

- Co-ordinates z_g and y_g of the centroid:

$$z_g = \frac{S_{y0}}{A} = \frac{\sum_{i=1}^{n} (\overline{z_i} + \overline{z_{i-1}}) \frac{dA_i}{2}}{A} \tag{A2a}$$

$$y_g = \frac{S_{z0}}{A} = \frac{\sum_{i=1}^{n} (\overline{y_i} + \overline{y_{i-1}})(dA_i/2)}{A} \tag{A2b}$$

- Sectorial area co-ordinates:

$$\omega_0 = 0 \tag{A3a}$$

$$\omega_{0i} = \overline{y_{i-1} z_i} - \overline{y_i z_{i-1}} \tag{A3b}$$

$$\omega_i = \omega_{i-1} + \omega_{0i} \tag{A3c}$$

- Mean value of the sectorial area:

$$\omega_{mean} = \frac{\sum_{i=1}^{n} (\omega_{i-1} + \omega_i)(dA_i/2)}{A} \tag{A4}$$

- Sectorial constants:

$$I_{y\omega} = I_{y\omega 0} - \frac{S_{z0} I_\omega}{A} = \sum_{i=1}^{n} (2\overline{y_{i-1}}\omega_{i-1} + 2\overline{y_i}\omega_i + \overline{y_{i-1}}\omega_i + \overline{y_i}\omega_{i-1}) \frac{dA_i}{6} - \frac{S_{z0} I_\omega}{A} \tag{A5a}$$

$$I_{z\omega} = I_{z\omega 0} - \frac{S_{y0} I_\omega}{A} = \sum_{i=1}^{n} (2\overline{z_{i-1}}\omega_{i-1} + 2\overline{z_i}\omega_i + \overline{z_{i-1}}\omega_i + \overline{z_i}\omega_{i-1}) \frac{dA_i}{6} - \frac{S_{y0} I_\omega}{A} \tag{A5b}$$

$$I_{\omega\omega} = I_{\omega\omega 0} - \frac{I_\omega^2}{A} = \sum_{i=1}^{n} ((\omega_i)^2 + (\omega_{i-1})^2 + \omega_i \omega_{i-1}) \frac{dA_i}{3} - \frac{I_\omega^2}{A} \tag{A6}$$

- Shear center coordinates $(I_y I_z - I_{yz}^2) \neq 0$:

$$y_s = \frac{I_{z\omega} I_z - I_{y\omega} I_{yz}}{I_y I_z - I_{yz}^2} \tag{A7a}$$

$$z_s = \frac{-I_{y\omega} I_y - I_{z\omega} I_{yz}}{I_y I_z - I_{yz}^2} \tag{A7b}$$

- Warping constant (I_w):

$$I_w = I_{\omega\omega} + z_s I_{y\omega} - y_s I_{z\omega} \tag{A8}$$

- Sectorial co-ordinate with respect to shear center:

$$\omega_{n(i)} = \omega_i - \omega_{mean} + z_s(\overline{y_i} - \overline{y_g}) - y_s(\overline{z_i} - \overline{z_g}) \tag{A9}$$

- Eccentricity of the shear center respect to the centroid:

$$y_0 = y_s - y_g \; z_0 = z_s - z_g \tag{A8}$$

- Warping modulus:

$$W_w = \frac{I_w}{\max(|\omega_n|)} \tag{A10}$$

- First moment of sectorial area (S_w):

$$S_{\omega 0} = 0 \tag{A11a}$$

$$S_{\omega i} = \frac{(\omega_{n(i-1)} + \omega_{n(i)}) dA_i}{2} + S_{\omega(i-1)} \tag{A11b}$$

Appendix B. List of symbols

Latin lower case letters

m	non-dimensional moment.
n	non-dimensional axial load
u	displacement along the x axis
v	displacement along the y axis
w	displacement along the z axis
x	longitudinal axis of the beam
y	symmetry axis of the cross-section
z	non symmetry axis of the cross-section

Latin upper case letters

B	bi-moment
C	internal
DOF	degrees of freedom
E	Young's modulus. external
U	upright
F	shear force
FE	finite element
I	second moment of area
K	matrix stiffness, stiffness coefficient, effective length coefficient
M	moment
N	axial force
P	generic point
S	beam-to-column joint stiffness, base-plate joint stiffness, first moment of area (section modulus)
SI	safety index
W	resistance elastic modulus

Greek lower case letters

α	load multiplier
β	equivalent uniform moment factor
γ	factor
φ	rotation
ρ	radius gyrator of inertia, non-dimensional rotation stiffness
θ	warping function
ω	sectorial area
δ	longitudinal displacement
χ	reduction factor
$\bar{\lambda}$	slenderness
σ	normal stress

Subscripts

b	beam
BC	beam–column
btc	beam-to-column connection
base	base-plate connection
cr	critical
db	distortional buckling
Ed	design value
eff	effective
F	flexural buckling
FT	flexural–torsional buckling

G	global
i	initial node
j	node of the beam element joint
LT	lateral torsional instability
M	material. moment
max	maximum
min	minimum
o	position of the centroid
Rd	design resistance
s	position of the shear center, service load
T	torsional buckling
t	uniform torsion
u	upright. ultimate load multiplier
w	warping
x	longitudinal axis of beam element
y	symmetry axis of the cross-section. yielding of the material
z	non symmetry axis of the cross-section
ω	sectorial area

Superscripts

6	analysis with a beam element formulation having 6DOFs per node
6+FT	6DOFs FE analysis combined with the flexural–torsional buckling
7	analysis with a beam element formulation having 7DOFs per node
BM	bi-moment contribution
E	elastic stiffness matrix
G	geometric stiffness matrix, global resistance check
SL	system length
SL+FT	system length combined with the flexural–torsional buckling
W	Wood's method
W+FT	Wood's method combined with the flexural–torsional buckling

References

[1] CEN, EN 15512, Steel static storage systems – Adjustable pallet racking systems – Principles for structural design, CEN European Committee for Standardization. 2009. pp. 137.

[2] Bernuzzi C, Gobetti A, Gabbianelli G, Simoncelli M. Unbraced pallet rack design in accordance with european practice. Part 1: selection of the method of analysis. Thin Walled Struct 2014 (submittedfor).

[3] Bernuzzi C. Gobetti A.. An innovative finite element formulation for analysis of beam element with thin-walled monosymmetric section. in preparation.

[4] Bernuzzi C. Gobetti A. Gabbianelli G. Simoncelli M.. Śiva-System of Incremental and vibration analysis: software for a finite element analysis for beam with warping influence. in preparation.

[5] Chen WF, Atsuta T. Theory of beam-Columns: vol. 2 Space behaviour and design. Mc Graw Hill; 1977.

[6] Turkalj G, Brnic J, Prpic-Orsic J. Large rotation analysis of elastic thin walled beam-type structures using ESA approach. ComputStruct 2003;81:1851–64.

[7] Battini JM. Co-rotational beam elements in instability problems. Stockholm. Sweden: Technical Report from Royal Institute of Technology Department of Mechanics; 2002.

[8] Bathe K, Wilson EL. Numerical methods in finite element analysis. Englewood Cliffs: Prentice-Hall; 1976.

[9] Werkle H. Finite element in der baustatik. Braunschweig-Wiesbaden: Vieweg; 2008.

[10] Zienkiewicz OC, Taylor RL. The finite element method. Oxford: Butterworth Heinemann; 2000.

[11] European Committee for Standardization. CEN EN 1990 – Eurocode 0 – Basis of structural design. CEN. December. 2005.

[12] Vlasov VZ. Thin walled elastic beams. 2nd ed.. Jerusalem: Israel Program for Scientific Transactions; 1961.

[13] Timoshenko SP, Gere JM. Theory of elastic stability. 2nd ed.. New-York: McGraw Hill; 1961.

[14] Bernuzzi C. Gobetti A. Gabbianelli G. Simoncelli M.. "Overview on the design of Pallet Beams for Steel Storage Pallet and Drive-in Rack Systems". in preparation.

[15] European Committee for Standardization CEN. Eurocode 3 – Design of steel structures – Part-1: General rules and rules for buildings. CEN European Committee for Standardization.

[16] Australian Standards. AS 4084 - Steel Storage Racking. AS Standards. Australia. 2012.

[17] Bernuzzi C, Gobetti A, Gabbianelli G, Simoncelli M. Warping influence on the resistance of uprights in steel storage pallet racks. J Constr Steel Res 2014;101:224–41.

[18] Wood RH. Effective lengths of columns in multi-story buildings-part 1 Effective lengths of single columns and allowance for continuity. Struct Eng 1974;52(7): 235–44.

[19] ECCS-European Convention for Structural Steelworks. Analysis and design of steel frames with semi-rigid joints. publication. 67. 1992.

[20] European Committee for Standardization CEN EN 10025: Hot rolled products of structural steels.

[21] Bernuzzi C, Pieri A, Squadrito V. Warping influence on the static design of unbraced steel storage pallet racks. Thin-Walled Struct 2014;79:71–82.